GEOLOGIJA 68/2, 123-145, Ljubljana 2025
© Author(s) 2025. CC Atribution 4.0 License

https://doi.org/10.5474/geologija.2025.006

Article

Evaluation of cut slope stability in the Lesser Himalaya of Nepal

Ocena stabilnosti vkopnih brežin v Nizki Himalaji v Nepalu

Krishna Kumar SHRESTHA[1], Kabi Raj PAUDYAL[1], Dinesh PATHAK[1], Alessandro FRANCI[2] & Prem Bahadur THAPA[3]*

[1]Central Department of Geology, Tribhuvan University, Kirtipur, Kathmandu, Nepal
[2]International Center for Numerical Methods in Engineering (CIMNE), Universitat Politècnica de Catalunya (UPC), Carrer Gran Capitán, UPC Campus Nord, Barcelona, Spain
[3]Department of Geology, Tri-Chandra Multiple Campus, Tribhuvan University,
*Corresponding author's e-mail: prem.thapa@trc.tu.edu.np

Prejeto / Received 9. 5. 2025; Sprejeto / Accepted 6. 6. 2025; Objavljeno na spletu / Published online 30. 7.2025

Key words: cut slope, slope stability, numerical modelling, evaluation and validation, Lesser Himalaya, Nepal
Ključne besede: vkopna brežina, stabilnost pobočja, numerično modeliranje, vrednotenje in potrjevanje, Nizka Himalaja, Nepal

Abstract

A spatial inventory of cut slopes in the central and western Lesser Himalaya of Nepal was prepared and characterised to evaluate their stability. The stability of these cut slopes is governed by the geotechnical properties of rock/soil together with slope geometry, groundwater conditions and human interventions. Numerous cut slope failures were observed in areas where slope geometry is modified for engineering developments such as roads, dams, powerhouses, industrial development, etc. Two modelling sites were evaluated using the Limit Equilibrium Method (LEM), Finite Element Method (FEM), and Particle Finite Element Method (PFEM). Pre-failure analyses using LEM and FEM under dry and saturated conditions revealed that the stability of the Lesser Himalayan hillslopes with considerable soil thickness is predominantly controlled by the depth of groundwater level (GWL). Slopes remain stable with a factor of safety (FoS)>1.3 when the GWL lies below 7 m from the surface and gradually become unstable as it approaches the surface. This trend for both slopes confirms that elevated groundwater during the rainy season is the major cause of frequent cut slope failures in the Himalayan regions. The comparison of FoS from LEM and Strength Reduction Factor (SRF) from FEM showed a strong cross-correlation (90–99 %), revealing minimal variation which affirmed the validity of the adopted modelling techniques used in this study. Post-failure simulations of these sites were further analysed using an innovative approach, the robust PFEM modelling technique, to compute the dynamic failure mechanism. Sensitivity analysis of both modelled sites showed that friction angle and cohesion are the most significant parameters for slope stability evaluation. Moreover, forward and back analyses indicated that computed results are in good agreement, thus depicting reliability and performances along with the model validation.

Izvleček

Za oceno stabilnosti vkopnih brežin v osrednjem in zahodnem delu Nizke Himalaje v Nepalu je bil pripravljen in karakteriziran prostorski popis. Stabilnost teh brežin je odvisna od geotehničnih lastnosti kamnin in tal, geometrije pobočja, hidrogeoloških razmer ter človekovih posegov v prostor. Na območjih, kjer je bila zaradi inženirskih posegov, kot so gradnja cest, jezov in elektrarn, spremenjena geometrija pobočja, so bila opažena številna porušenja vkopnih brežin. Z uporabo metode mejnega ravnotežja (LEM), metodo končnih elementov (FEM) in metodo delnih končnih elementov (PFEM) sta bili izbrani dve lokaciji modeliranja. Analize, izvedene z metodama LEM in FEM v suhih in nasičenih pogojih so pokazale, da je stabilnost pobočij v Nizki Himalaji, prekritih z večjo debelino tal, pretežno odvisna od globine nivoja podzemne vode (GWL). Pobočja ostajajo stabilna s faktorjem varnosti (FoS) >1,3 kadar gladina podzemne vode (GWL) leži več kot 7 m pod površjem in postopoma postajajo vedno bolj nestabilna, ko se nivo vode približuje površju. Ta trend je opazen pri obeh izbranih pobočjih in potrjuje, da je povišana gladine podzemne vode v obdobju deževne dobe glavni vzrok pogostih porušitev pobočij v himalajski regiji. Primerjava faktorjev varnosti izračunanih z metodo LEM ter faktorja zmanjšane trdnosti (SRF) pridobljenega z metodo FEM je razkrila močno medsebojno korelacijo (90–99 %), kar kaže na minimalne razlike in potrjuje zanesljivost uporabljenih modelirnih tehnik v tej študiji. Simulacije po porušitvi na teh območjih so bile dodatno analizirane z uporabo inovativnega robustnega pristopa z PFEM modeliranjem za izračun dinamičnega mehanizma porušitve. Analiza občutljivosti obeh modeliranih območij je pokazala, da sta trenje in kohezija ključna parametra za oceno stabilnosti pobočij. Poleg tega so druge izvedene analize pokazale dobro ujemanje pridobljenih rezultatov, kar potrjuje zanesljivost modela, njegovo učinkovitost ter veljavnost.

Introduction

Mass movements such as landslides, debris flow and cut slope failures are significant hazards and risks in the Lesser Himalaya of Nepal, particularly during the rainy season. These events are exacerbated by weak and fractured lithologies, intense seasonal rainfall, active tectonics and increasing human interventions. Average altitudes of this region vary from 300 to 3500 m (Groppo et al., 2023), and it is the most populated region in the Himalaya that comprises sedimentary and less metamorphosed rocks (Upreti, 1999). Impacts of active tectonics, extensive human intervention and rapidly growing infrastructure development in this region are extremely exacerbating the landslides and cut slope failures. Most of the infrastructures concentrated near the road, which declines as a function of distance from the road network, justifies the significance of the road in terms of socio-economic development (Rawat & Sharma, 1997).

The occurrence of cut slope failures to large-scale landslides is frequent in the Lesser Himalayan Terrain of Nepal (e.g., Hasegawa et al., 2009; Phuyal et al., 2022; Thapa et al., 2023; Phuyal et al., 2025). Major highways in Nepal often traverse through river valleys and steep mountainous regions where numerous cut slopes of varying geometries are highly susceptible to failure during rainfall and earthquakes. About 46 % of the Prithvi Highway (NH04) runs through hillsides with multiple cut slopes. The Krishnabhir landslide (83 km west of Kathmandu) in 2000 blocked the Prithvi Highway for over two weeks, causing a shortage of daily commodities (Maskey, 2016) in the capital city. Similarly, the Jogimara landslide (90 km west of Kathmandu) also obstructed the highway for 10 days (Upreti & Dhital, 1996). These locations were recurrently affected by landslides for almost a decade, and the annual blockages during the monsoon season caused repeated disruptions to public and local transportation networks. The Jure landslide in 2014 along the Araniko Highway killed 156 people and damaged 2 km of road (Panthi, 2021). Over 4,000 landslides and cut slope failures occurred between 1971 and 2020, causing 5,000+ deaths, averaging 111 annually (Adhikari & Gautam, 2022). In 2023, 45 deaths were recorded, while in 2024, 343 deaths and 48 missing cases occurred by the end of the monsoon. Unusual intense rainfall from 26 to 28 September 2024 triggered more than 500 landslides and cut slope failures along the Prithvi Highway alone, causing severe disruptions and 35 fatalities in a single incident. These data indicate the vulnerability of highways to slope failures in mountainous regions underscoring the urgent need for comprehensive slope stability assessment to reduce the socio-economic impacts.

Geological structures, active seismic zones, steep topography, seasonal rainfall (hydro-meteorological), and increasing anthropogenic activities are the major causes of mass movement in weak areas like in the Lesser Himalaya (Varnes, 1958; Gerrard, 1994; Upreti, 1999; Shrestha et al., 2004; Dahal et al., 2006; Dahal & Hasegawa, 2008; Singh, 2009; Haigh & Rawat, 2011; Devkota et al., 2013; Regmi et al., 2013; Rahman et al., 2014; Dahal, 2014; Pathak, 2016; Marc et al., 2019; Dikshit et al., 2020; Shrestha et al., 2023). These appear in the form of earth flow, debris, bulging, rock fall, avalanches and so on (Varnes, 1978; Cruden & Varnes, 1996; Hungr et al., 2014). Infrastructure development in this region requires natural slopes subject to cutting to create space for roads, hydropower facilities, industries, railways, airports and canals, resulting in cut slopes of varying scales (DoR, 2007; Sutejo & Gofar, 2015). Geo-environmental factors like slope geometry, lithology, soil depth, weak band, groundwater condition, drainage density and proximity to faults are the key factors to control the stability of excavated cut slopes (Wyllie & Mah, 2004; Singh et al., 2020).

Defective engineering techniques in changing the slope geometry, torrential rainfall (Dahal et al., 2006), long exposure to the atmosphere, the presence of weak bands, rapid weathering, shallow groundwater, lack of surface drainage and dynamic loading frequently cause roadside failures. Various incidents of landslides from small to large scales along the major highways of Nepal were reported (Schuster & Hubl, 1995; Upreti & Dhital, 1996; Martin, 2001; Bhattarai et al., 2004; Hearn, 2011; Dahal, 2014; Thapa, 2015; Regmi et al., 2016; Hearn & Shakya, 2017; Vuillez et al., 2018; Pant and Acharya, 2021; Pradhan et al., 2022; Robson et al., 2022; Pudasaini et al., 2024; Shrestha et al., 2023; Pokhrel et al., 2024; Robson et al., 2024; Sapkota & Timilsina, 2024; Phuyal et al., 2025, etc.). Within the different road sections in the Lesser Himalaya terrain of Nepal, various methods of analytical, conventional and numerical modelling techniques have been used to analyse the cut slope stability on soil and rock by different researchers (Ray & Smedt, 2009; Pathak, 2014; Dhakal & Acharya, 2019; Shrestha et al., 2023; Acharya & Dhital, 2023; Poudyal et al., 2024).

Cut slope stability evaluation utilises various conventional and numerical modelling approaches through the Limit Equilibrium Method (LEM)

and the Finite Element Method (FEM). LEM often uses the "method of slices" to calculate the Factor of Safety (FoS) based on driving and resisting forces (Morgenstern & Sangrey, 1978; Nian et al., 2012; Burman et al., 2015; Deng et al., 2017). FEM, on the other hand, offers a more complex approach which incorporates stress-strain behaviour and material properties to analyse slope stability (Griffiths & Lane, 1999; Burman et al., 2015). The majority of cut slope stability assessments in the Nepal Himalaya have relied on field investigations, rock mass classification and calculation of FoS by conventional techniques. However, few studies have attempted to evaluate cut slope stability in Nepal using numerical modelling techniques for comprehensive analyses (e.g., Kharel & Acharya, 2017; Khatri & Acharya, 2019; Shrestha et al., 2023). Thus, the present study has integrated computational techniques of numerical modelling in evaluating the cut slope stability within the Himalayan terrain. Based on the spatial inventory of cut slopes in the Lesser Himalaya of central and western Nepal, two cut slopes have been chosen for detailed study, as they represent typical slides in their respective regions and have seriously impacted the socio-economic conditions of the community that depends entirely on the roads passing through them. The modelling approaches of LEM, FEM and the particle finite element method (PFEM) have been implemented to compute the pre-failure and post-failure mechanisms of the respective slopes. The results obtained through these techniques were validated based on the field evidence and simulated results of the computed models.

Study area

The study area is situated in the western and central Nepal Himalaya, bounded by latitudes 27°48'52" N to 27°49'12" N and longitudes 83°17'33" E to 86°13'11" E (Fig. 1). The areal coverage of the study area is about 17,500 km^2 and lies in the adjoining regions of the major cities Pokhara and Kathmandu, with elevations ranging from 230 m to 3,780 m. However, the actual investigation is focused primarily along the road corridors, as the majority of cut slopes are located adjacent to road alignments. The total length of road sections assessed in this study is approximately 2000 km, encompassing both primary and secondary highway networks. The geomorphology of this region is largely shaped by metamorphic and meta-sedimentary rocks of the Lesser Himalaya. The area has experienced significant uplift and erosion, which has shaped a complex geo-environment, forming various geomorphic landforms. The major physiographic divisions, namely the Mahabharat Range and Midland Zone, are the major landform units in this region. The Mahabharat Range is a distinct high mountain belt north of the Indo-Gangetic Plain, while the Midland Zone features a relatively subdued landscape typically covered with residual, colluvial and alluvial deposits. The characteristics of landform conditions combined with extensive anthropogenic activities predispose the region to frequent landslides and slope failures during the summer monsoon season.

Geological setting and spatial distribution

Geologically, the study area lies within the Lesser Himalayan Zone of Nepal and is bounded by two major thrust sheets of the Himalaya: the Main Boundary Thrust (MBT) to the south and the Main Central Thrust (MCT) to the north (Fig. 1). This region consists of two distinct metamorphic zones that include the low-grade Lesser Himalayan metasediments and the high-grade Lesser Himalayan Crystallines (Gansser, 1974). This zone features abundant faulting and folding as its primary geological structures (Upreti, 1999; Dhital, 2015). The main rock types in this area comprise slate, phyllite, schist, quartzite, dolomite and limestone, with some intrusions of granites and meta-basic rocks. The differential strengths of rock strata with highly folded and faulted geo-environments make the region particularly susceptible to landslides and cut slope failures. The prediction of slope failures and landslides together with assessment of mitigative measures becomes essential because of the complex slope failure process and limited understanding of underlying mechanisms which are typical problems in mountainous regions, especially along the hill-cut slope of the Lesser Himalaya (Singh et al., 2008; Hasegawa et al., 2009).

A cut slope inventory database has been developed from various road sections of major highways within the study area of central and western Nepal. Two specific sites were selected for further detailed investigations, as they are the recurring slope failures annually and have considerable socio-economic impacts: the Kokhe Slide in Gorkha District (Site-1: 28°01'35"N, 84°40'13"E) along the Gorkha-Arughat rural road and the Udipur Slide in Lamjung District (Site-2: 28°10'51"N, 84°25'43"E) along the Dumre-Besishahar-Chame Highway (NH25) of Nepal (Fig. 1). Both slides are recurrently triggered during the monsoon season, influenced by shallow groundwater tables, weak and weathered lithology typical of slopes in the

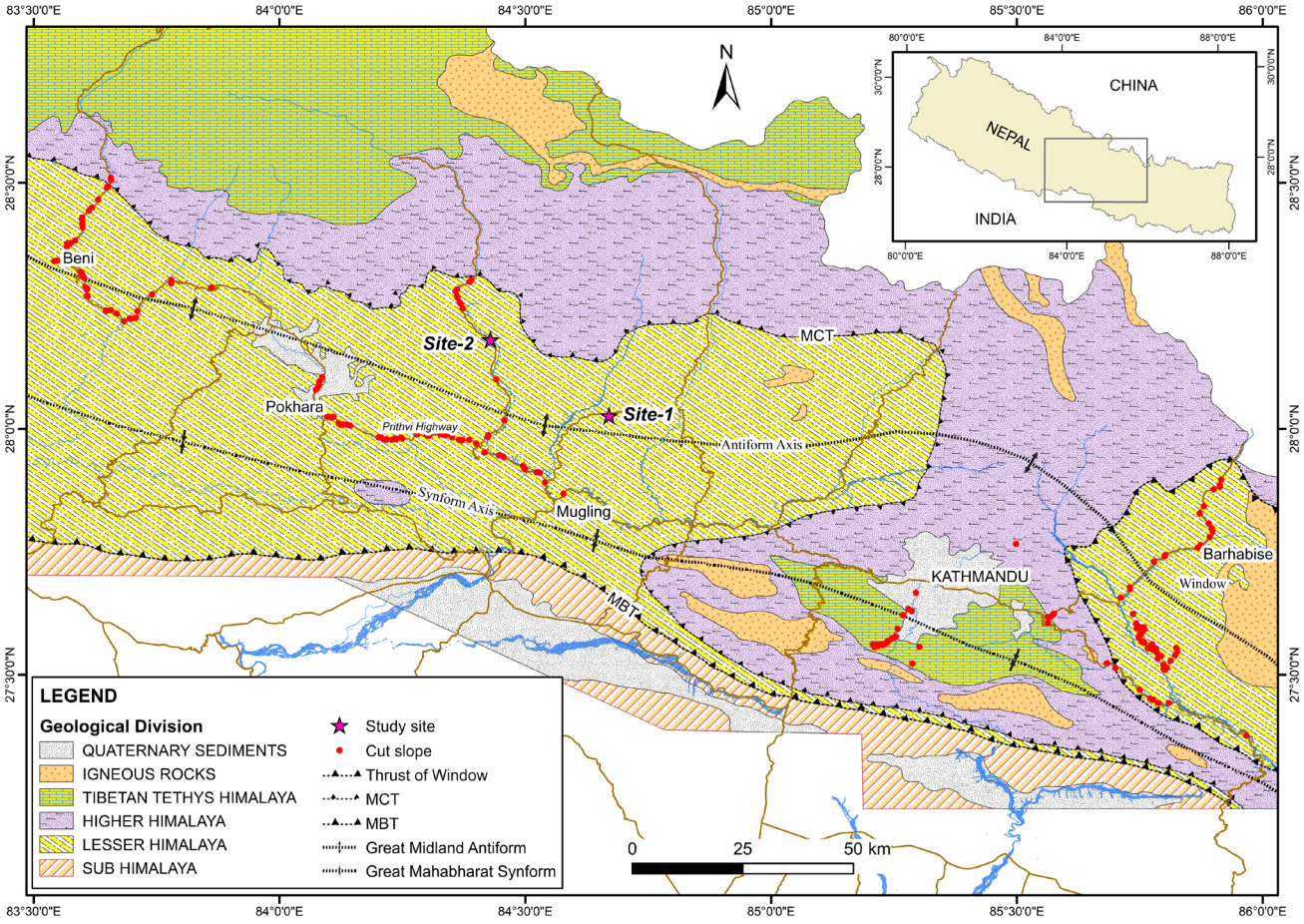

Fig. 1. Geological setting (modified after Dhital, 2015) and spatial distribution of cut slopes in the study area.

Lesser Himalaya, inadequate drainage, and various anthropogenic disturbances. The slide at Site-1 initiated before 2009 and is still posing threats to public transport during the monsoon of every year as progressive sliding occurs annually. The major failure at Site-2 occurred in July 2022 and swept away the 90 m road section downhill and is reactivating during the monsoon of every year. Detailed investigations are based on typical slope geometries, rapidly rising groundwater tables and recurrent failures with a documented history that have a direct impact on public transportation. Findings from these slopes can be applied to many other slides with similar features in terms of geometry, lithology, groundwater conditions, precipitation patterns and socio-economic impacts.

Cut slopes and site characteristics

The characteristics of cut slopes in the Lesser Himalaya are influenced by slope geometry, lithology, weathering and hydrogeological conditions (Upreti & Dhital, 1996; Wyllie & Mah, 2004; Dahal et al., 2008; Phuyal & Thapa, 2023; Shrestha et al., 2023). Cut slope failures in the study area are often observed on higher and steeper slope gradients experiencing more gravitational forces that have increased the shear stress exceeding the soil strength (Fig. 2a). Improper and non-engineered methods of excavation during construction without due consideration of local geology are significant contributors to slope failures.

Many steep and high cut slopes formed in heavily weathered rocks are in a marginal stable state even under dry conditions. During rainfall, these materials become saturated and fail due to excessive pore pressure development (Fig. 2b). Failures often occur in areas with highly jointed, fractured, folded or faulted rock masses within the Lesser Himalaya (Fig. 2c, d).

Every year, high and prolonged precipitation during the monsoon saturates the soil and increases pore water pressure therein. This reduces the effective stress and shear strength of the soil and leads to instability (Terzaghi, 1943; Craig, 2004; Duncan & Wright, 2005). Tensional cracks developed at the crown of the slope create a path for water to percolate easily into the slope and aggravate the failure mechanism (Fig. 2e). Residual soil found along the road section with unprotected higher slope height and steeper gradient is susceptible to failure during the wet season (Fig. 2f).

Fig. 2. Cut slope characteristics in the Lesser Himalayan Zone of western and central Nepal: (a) weak rock exposure and steep cut slope failed during heavy rainfall along the Prithvi Highway, Tanahun, (b) completely weathered high slope along the Kanti Lokpath, Lalitpur, (c) rock blocks over loose materials failed along the Pushpalal Highway, Kaski, (d) folded rock showing numerous discontinuities prone to failure at Dolakha, (e) a translational slide along the Kathmandu-Melamchi Highway, Sindhupalchowk, and (f) a failed residual soil slope due to slope modification for highway expansion along the Prithvi Highway, Dhading.

The cut slopes failure at Site-1 consists of the residual soil formed from the phyllite rock of the Kuncha Formation. The lithology in this area is psammitic phyllite, which is characterised by alternating layers of crenulated micaceous material comprising microfolds and a quartz-rich layer embedded within the fine-grained matrix of well-foliated mica minerals. This type of phyllite consists of quartz, K-feldspar, and muscovite as primary minerals, whereas tourmaline, biotite, opaque minerals, oxides and clay minerals as accessory minerals (Silwal et al., 2024). Sericitisation and

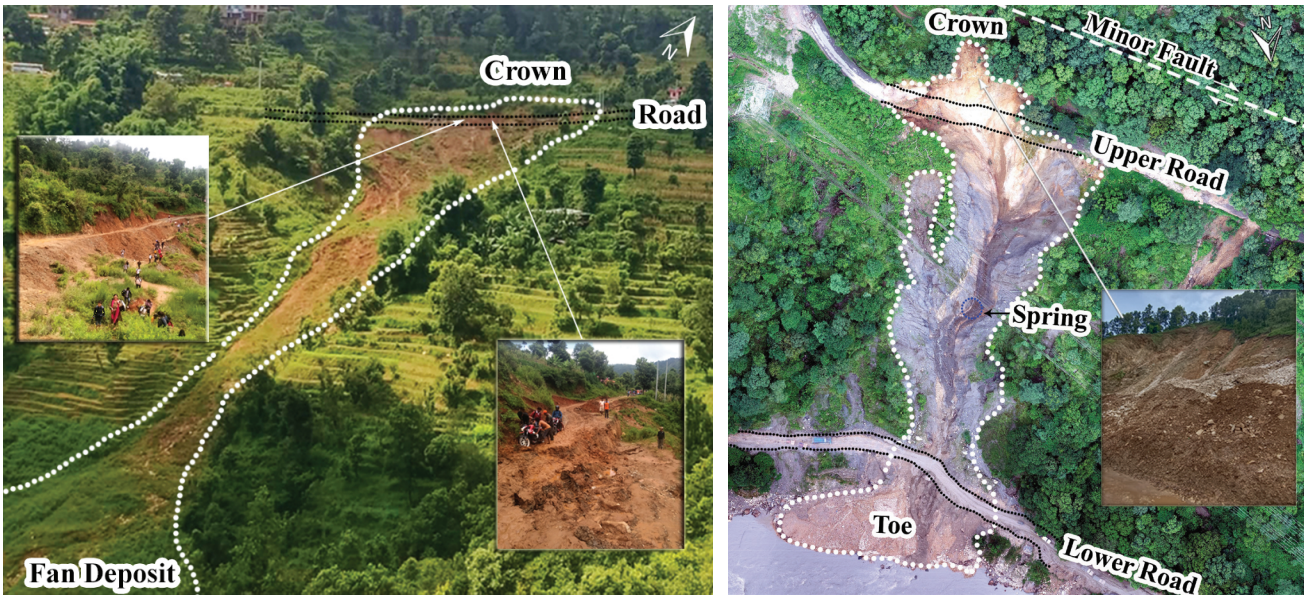

Fig. 3. Characteristic features of the modelling sites: (a) Site-1, the Kokhe Slide, inset shows the road conditions within the slide-affected section, (b) Site-2, the Udipur Slide, inset shows the slope section above the road.

alteration effects are very common in this type of rock and are well observed in the slope materials (Fig. 3a). Mineral composition and textural features (e.g., foliation, cracks, alterations) aid in classifying rock strength and weathering grades, which in turn help estimate geotechnical parameters (e.g., unit weight, Young's modulus, Poisson's ratio). Furthermore, the presence of micaceous minerals (e.g., sericite, clay) indicates weak rock mass that are associated with observed failure mechanisms.

The cut slope failure at Site-2 lies under the Fagfog Quartzite of the Lower Nawakot Group, which is highly fractured and thinly foliated with poor rock mass quality (Panthi, 2006). The section above the road is characterized by highly fractured and weathered quartzite, and the lower section contains thick colluvium. A minor fault is expected in this area, as seen by the high fracture frequency observed in the quartzite rock (Fig. 3b).

Data and methodology

Representative soil and rock samples from the slope failure scarp and adjacent exposures of the selected sites 1 and 2 were collected for laboratory testing to determine geotechnical properties. Unit weight (γ), cohesion (c), friction angle (ϕ), Young's modulus (E), Poisson's ratio (ν) and density (d) are the required input parameters for slope stability evaluation (Table 1).

Table 1.Geotechnical parameters of Site-1 and Site-2.

Parameters	Site-1				Site-2			
	Soil		Rock mass		Soil		Rock mass	
	DC*	SC**	DC	SC	DC	SC	DC	SC
Unit weight (γ), kN/m^3	17.2	18.4	26	22.81	17.0	19.6	26	27.5
Cohesion (c), kPa	16	4	42	35.8	40	20	200	185
Friction Angle (φ), °	22	14	38	32	28	14	35	31
Young's Modulus (E), kPa	40,000	40,000	52,000×10^3	52,000×10^3	400,000	400,000	36,000×10^3	36,000×10^3
Poisson's Ratio (ν)	0.4	0.4	0.23	0.23	0.30	0.30	0.25	0.25
Density (d) (kg/m^3)	1753	2331	-	-	1733	2180	-	-

***Note**: *DC = Dry condition, **SC = Saturated condition*

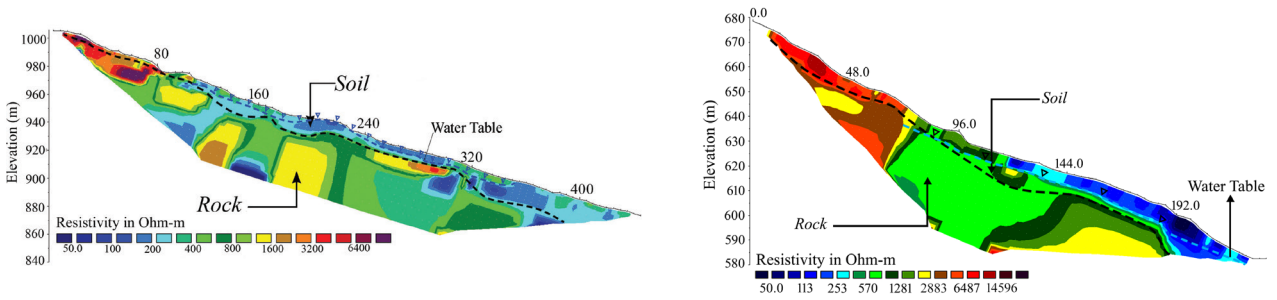

Fig. 4. Geophysical survey for subsurface investigation by electrical resistivity tomography: (a) Site-1 and (b) Site-2.

Field investigation of each specific site was carried out in detail using a Total Station (TS) survey for generating the hill slope profiles and a geophysical survey using Electrical Resistivity Tomography (ERT) for delineating sub-surface geological layers and identifying groundwater positions, which are important controlling factors in model development and slope stability analysis (Loke, 2004; Loke et al., 2013; Cardarelli & Fischanger, 2006; Panda et al., 2023). The interpretation of ERT correlates the variations in resistivity with different subsurface materials and conditions, such as lithology, moisture content and the groundwater level (Singh et al., 2014). Interpretative models derived from the processed tomograms of the slopes at sites 1 and 2 were integrated into slope-section profiles to evaluate cut slope stability (Fig. 4).

Modelling methods

Numerous advanced numerical techniques, encompassing continuum, discontinuum, and hybrid methods, are available for soil and rock slope stability analyses (Griffiths & Lane, 1999; Cheng et al., 2007; Zheng et al., 2014; Sharma et al., 2017). Numerical modelling of two cut slope failures (Kokhe and Udipur) was evaluated using Slide v.6.0 and Phase2 v.8.0, followed by a comparative analysis of Factor of Safety (FoS) under varying input conditions. Moreover, both sites were simulated utilising the multi-physics simulation framework "GiD" interface equipped with the Kratos platform. Input parameters for these simulations were also determined in the laboratory as per ASTM standards.

The numerical modelling processes involved a series of analytical computation workflows: defining problems based on site conditions, selecting the method, creating numerical models, computing outcomes and interpreting & validating results (Fig. 5). LEM and FEM modelling have evaluated the pre-failure state of cut slopes, and their post-failure mechanism has been analysed by Particle Finite Element Method (PFEM).

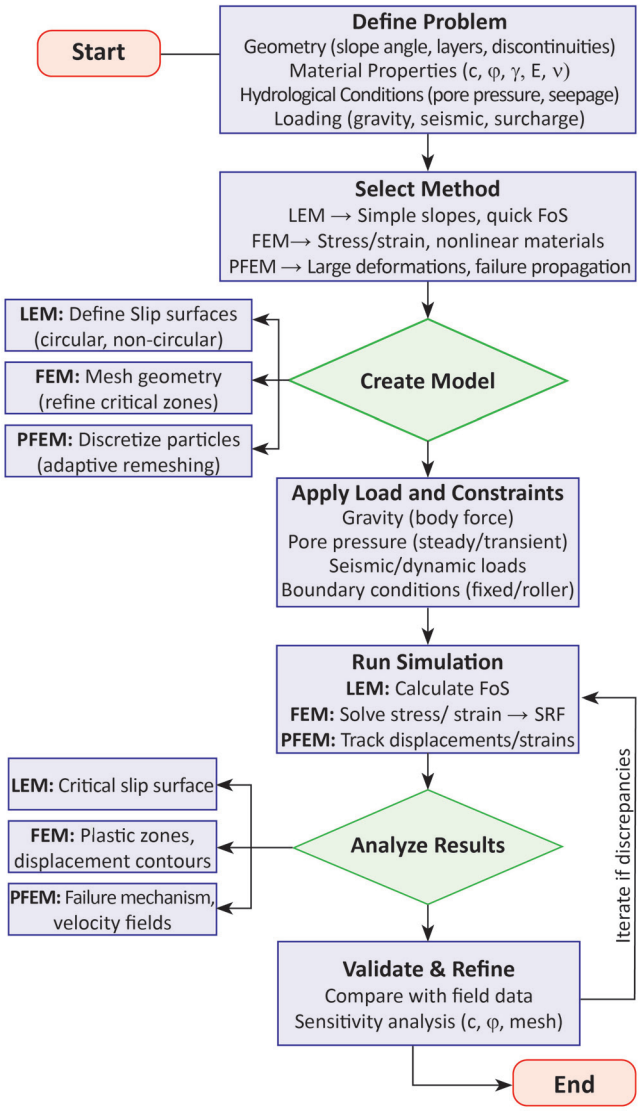

Fig. 5. Methodological framework for cut slope stability evaluation.

Model setup and computation

Numerical modelling of cut slopes involves slope behaviour simulation under various conditions to assess stability and failure modes (Singh et al., 2008). The model setup was performed by defining the geometry of the slope, assigning material properties, and applying boundary conditions (Fig. 6). The model geometry has encompassed the

actual slope, including its height and angle. Triangulated meshes were generated throughout the slope model with finer meshes around high-stress gradients and failure slip surfaces.

The GLE/Morgenstern-Price method (Slide v.6.0) was used in the LEM model to determine the safety factors in both dry and saturated conditions for evaluating the slopes in two different geo-environments. In addition, the same slope was computed by the FEM technique using Phase^2 v.8.0. The FEM model was discretised using six-noded triangular meshes of 3,000 elements under gravitational loading for dry and saturated conditions. Boundary conditions significantly influence slope stability analyses in numerical modelling (Chugh, 2003). Therefore, appropriate selection of boundary conditions is essential for reliable numerical modelling, which has been considered in this study.

After model setup with defined boundary conditions, assigned material properties and hydraulic parameters, simulations were conducted for varying groundwater levels. The variation of the FoS was evaluated in terms of fluctuating groundwater levels to identify the critical failure surface due to pore water pressure during rainy seasons. A plane strain analysis was further applied by selecting metric units and using the Gaussian elimination solver for accuracy purposes. The stress analysis was performed with a maximum of 500 iterations and a tolerance level of 0.001 to ensure convergence. The gravity loading was applied to the created model, and meshes were generated using a six-noded graded triangle as recommended by Komadja et al. (2020). Before running the simulation, the base and the right boundary of the model were restrained in both horizontal (X) and vertical (Y) directions to prevent movement. The model slope face was kept unrestrained to allow free deformation during numerical modelling.

The Limit Equilibrium Method (LEM) is a method of slices widely used for assessing slope stability because of its simplicity and user-friendliness. It derives FoS with respect to force and moment equilibrium. LEM analyses a slope by cutting it into fine slices and applying appropriate equilibrium equations (equilibrium of forces and/or moments) to calculate the FoS (Matthews et al., 2014). The common methods of LEM analysis are Ordinary/Fellenius (Fellenius, 1936), Bishop simplified (Bishop, 1955), Lowe and Karafiath (Lowe & Karafiath, 1965), GLE/Morgenstern-Price (Morgenstern & Price, 1965), Spencer (Spencer, 1967), Janbu Simplified and Janbu Corrected (Janbu, 1954), and Corps of Engineer #1 and #2 (USACE, 2003). Among these, the Morgenstern-Price (M-P) method (1965) and Sarma's method (1973) are advanced ones that account for both force and moment equilibrium and improve the accuracy of FoS on a factual basis. The M-P method involves complex equations, and different forms can be found depending on the assumptions made. The FoS in the Morgenstern-Price method is expressed as (Eq. 1) (Fan et al., 2021):

$$FoS = \frac{\int (c' + (\sigma - \mu)\tan\phi')\sec\alpha\, d_x}{\int \tau d_x} \qquad (1)$$

where, c' = effective cohesion, ϕ= effective angle of internal friction, σ = total normal stress on the base of the slice, μ = pore water pressure on the base of the slice, α= inclination of the base of the slice, and τ= shear stress on the base of the slice

The Finite Element Method (FEM) is an advanced computational technique which enhances traditional LEM by providing a higher degree of realism and deformation visualisations of materials (Matthews et al., 2014). FEM provides insights into stress, strain and displacement, which makes it a fundamental tool for analysing the deformation behaviour of slope materials (Cheng

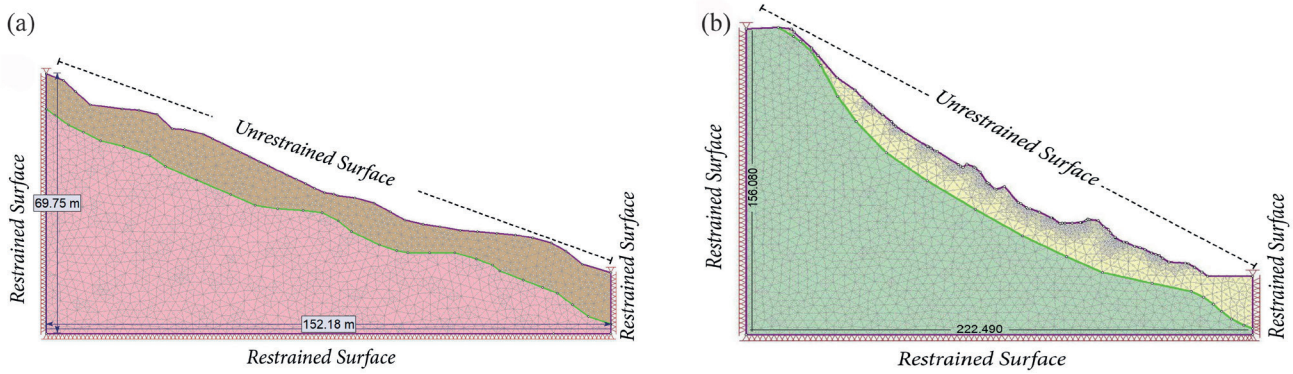

Fig. 6. Numerical model setup with mesh and boundary conditions: (a) Site-1 and (b) Site-2.

et al., 2007; Burman et al., 2015). FEM offers several advantages over LEM in slope stability analysis (Griffiths & Lane, 1999) as it does not require prior assumptions regarding the shape and location of the failure surface (Dawson et al., 1999). In this method, failure naturally emerges along a surface where material strength is deficient of resisting applied shear stresses. In FEM, the Shear Strength Reduction (SSR) technique has been applied to the Mohr-Coulomb criterion using Phase^2 to determine the Strength Reduction Factor (SRF).

The Particle Finite Element Method (PFEM) is a robust numerical technique which enables the solution of multi-physics problems involving extensive domain deformations (Oñate et al., 2004; Oñate et al., 2011). The PFEM model enables domain particles to move through space using Lagrangian dynamics while nodal variables determine their physical properties (e.g., density and viscosity) throughout the entire simulation period. The algorithm generates dynamic meshes through Delaunay triangulation and alpha shape scheme processes to prevent mesh distortion (Oñate et al., 2011).

The Navier–Stokes equations describe the fluid body motion and are governed by (Eq. 2 & 3). These equations relate the velocity u = u(x, t) and the Cauchy stress tensor σ = σ(x, t) through principles of momentum balance and mass conservation (Cremonesi et al., 2020) by:

$$\rho \frac{D\mathrm{u}}{Dt} = \mathrm{div}\,\sigma + b \quad \text{in } \Omega_t \times (0,T) \tag{2}$$

$$\frac{D\rho}{Dt} + \rho\,\mathrm{div}\,\mathrm{u} = 0 \quad \text{in } \Omega_t \times (0,T) \tag{3}$$

where, ρ(x) represents the fluid density, b(x, t) denotes external body forces per unit mass, and D/Dt is the material time derivative. A Lagrangian technique reduces the total time derivatives to a local time derivative and vanishes the convective factor in the governing equations. This characteristic is inherent in Lagrangian methods like the Particle Finite Element Method (Idelsohn et al., 2008; Idelsohn & Oñate, 2010; Franci et al., 2020).

The PFEM is capable of solving complex fluid-solid interaction problems and deformation mechanics. It is particularly useful in post-failure landslide analysis as it efficiently deals with extensive deformations, fragmentation and fluid-solid interactions. Both modelling sites (Site-1 and Site-2) were simulated in PFEM in terms of two-phase system based on distinct layers of materials identified from ERT and borehole data. The upper soil layer shows plastic behaviour under saturated conditions, whereas the underlying solid rock mass serves as a rigid and non-deforming base in the model. For Site-1, the saturated soil mass was modelled with a density (d) of 2331 kg/m^3, an internal friction angle (ϕ) of 14°, and cohesion (c) of 4 kPa, which were used as input parameters for the numerical computations.

Results and discussion

Limit Equilibrium Method (LEM)

The rigorous M-P method is an advanced and highly reliable method that satisfies both force and moment equilibrium (Zheng, 2012; Fan et al., 2021; Shrestha et al., 2023). This method has been adopted in the present modelling process. The safety factors of Site-1 were calculated under different conditions by considering fluctuations in the groundwater level of this area using this method, which is appropriate for analysing circular slip surfaces (Fig. 7). The analysis yielded a FoS of 1.42 under normal dry conditions (Fig. 7a), which is above the recommended minimum FoS of 1.25 for cut slopes, indicating a stable slope. Three different groundwater scenarios were analysed with varying depths of 7.0 m, 1.5 m and 0.5 m below the existing groundwater level (GWL). The calculated FoS values for these three different GWLs are 1.25, 0.97 and 0.87, respectively (Fig. 7b, c, d). Higher FoS values were observed with deeper GWL, and FoS decreased under elevated GWL, which corroborates the frequent cut slope failures observed during the rainy seasons.

According to the precipitation records from the Department of Hydrology and Meteorology (DHM, 2024), Nepal, the average annual precipitation at Site-1 is 254.88 mm. A transient analysis of this site for 24 hours with 250 mm of rainfall calculated a FoS of 1.18 after the implementation of gabion walls along with a three-stage drainpipe installation, representing the critical situation of slope during heavy rainfall (Fig. 7e). Considering the same rainfall condition with added static loading of 20 kN/m^2 and seismic loading of 0.17 g (horizontal) and 0.08 g (vertical), the calculated FoS is 1.10, which is still above the unity, indicating the marginal stability of slope (Fig. 7f) in the extreme conditions of loading too. There is a 42.98 % variation in FoS for Site-1 while transitioning from dry to saturated conditions.

The LEM analysis by M-P method for Site-2 has shown that the FoS in dry condition is 1.18

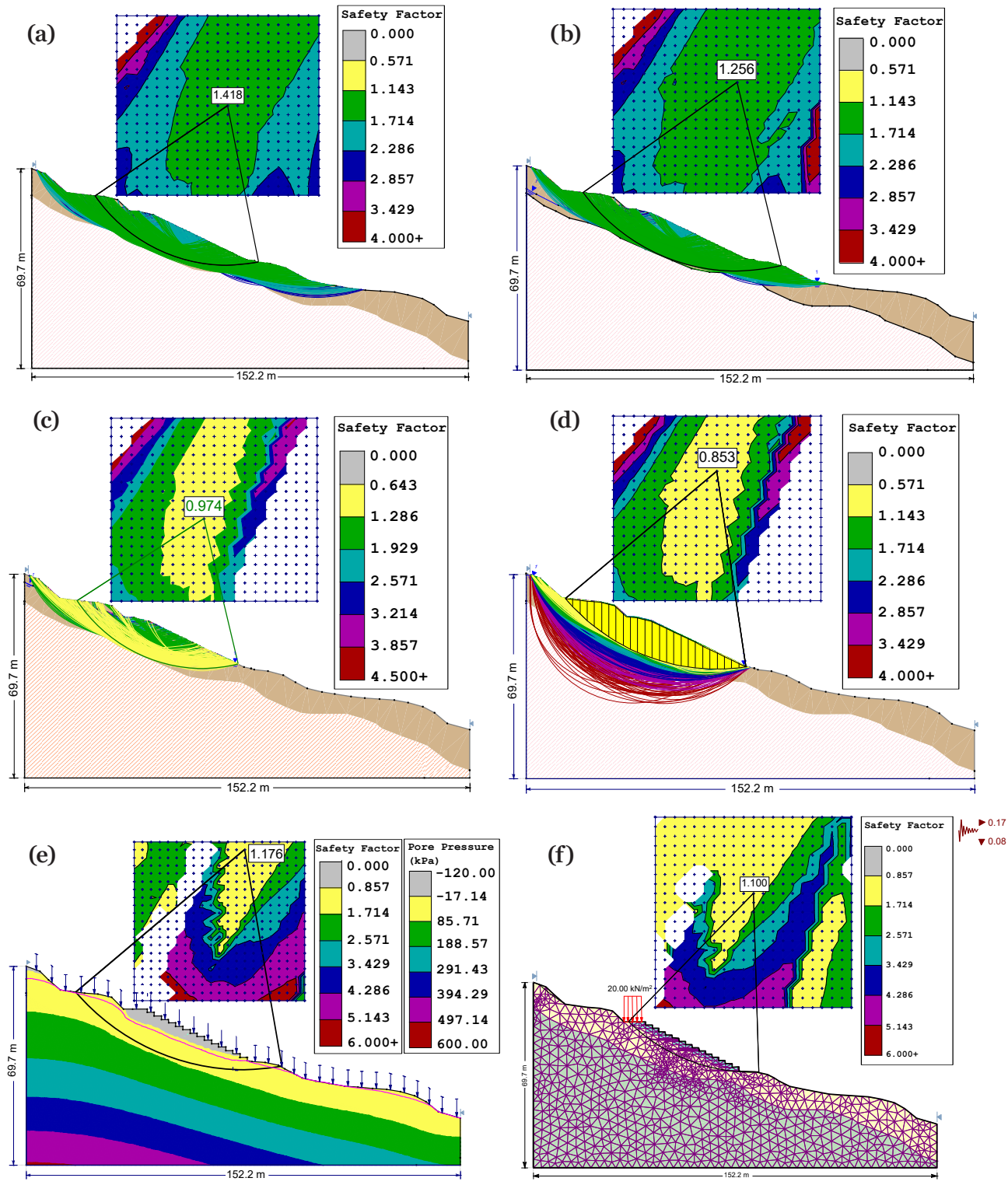

Fig. 7. Limit equilibrium stability analysis of Site-1: (a) dry condition, (b) GWL at 7 m, (c) GWL at 1.5 m, (d) GWL at 0.5 m, (e) transient analysis for 24 hours with 250 mm rainfall, (f) transient analysis with static loading of 20 kN/m^2 and seismic loading of 170 g (horizontal) and 80 g (vertical). (Note: The scale for all figures is same as given in Fig. 7a)

(Fig. 8a), which significantly declines to 0.41 under saturated condition (Fig. 8b). This slope exhibits marginal stability under dry conditions and ultimately transitions into an unstable state in saturated conditions. A variation of 66 % is found in the FoS for this slope when changing from dry to saturated conditions.

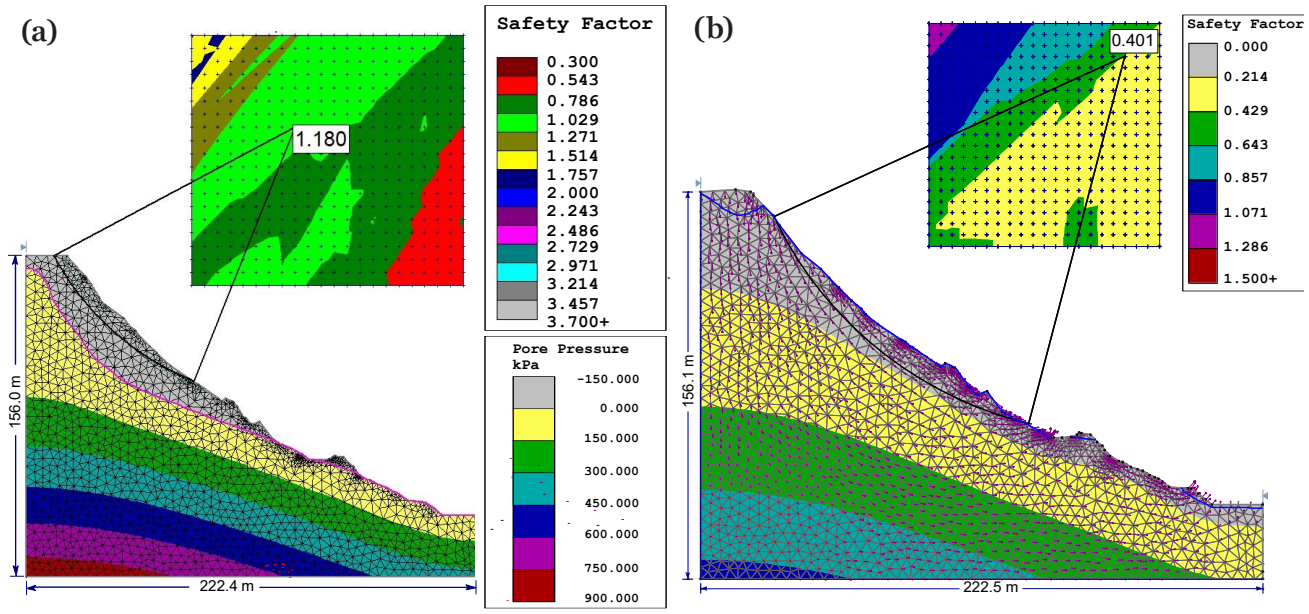

Fig. 8. Limit equilibrium stability analysis of Site-2: (a) dry condition, (b) saturated condition.

Finite Element Method (FEM)

The FEM analysis for Site-1 calculated an SRF of 1.45 under dry conditions, indicating a stable slope state. In saturated conditions, the SRF decreased to 0.82 (Fig. 9a-d), which has predicted the critical failure probability. These two conditions for Site-1 clearly show a 43.44 % change in safety factor when the slope gets saturated. Similarly, for Site-2, SRF under dry conditions is 1.15, showing a marginal stability of slope. This safety factor changes to 0.39 under saturated conditions. This change in FoS between two conditions is 66.08 %, which is very critical in terms of slope instability.

The maximum shear strain values at both slope sites have shown that elevated pore water pressure strongly influences slope materials to destabilise. The maximum shear strain at Site-1 increased from 0.0105 to 0.0315 on changing the scenario from dry to saturation, thereby showing a 57.5 % increase in slope material deformation (Fig. 9a, c). Likewise, Site-2 experienced a maximum shear strain of 0.00386 under dry and 0.009 under

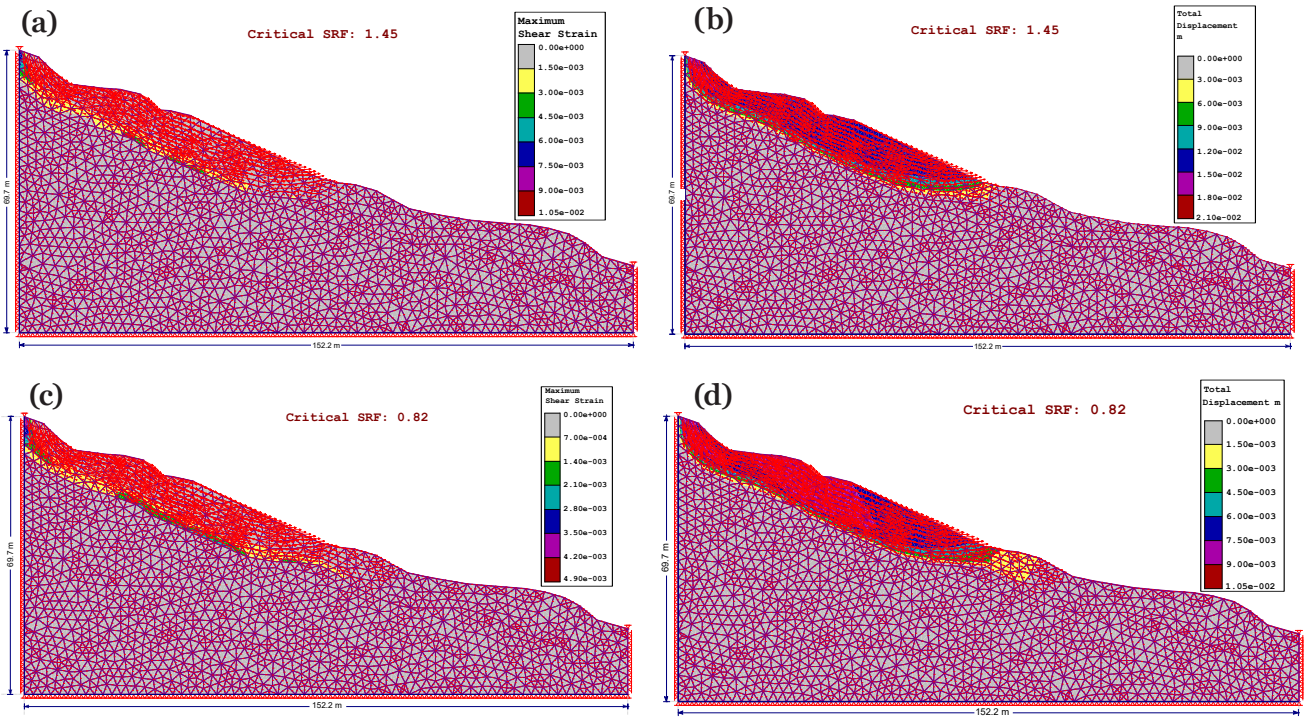

Fig. 9. Maximum deformation vectors at Site-1 under dry conditions: (a) shear strain, (b) total displacement and saturated conditions: (c) shear strain, (d) total displacement.

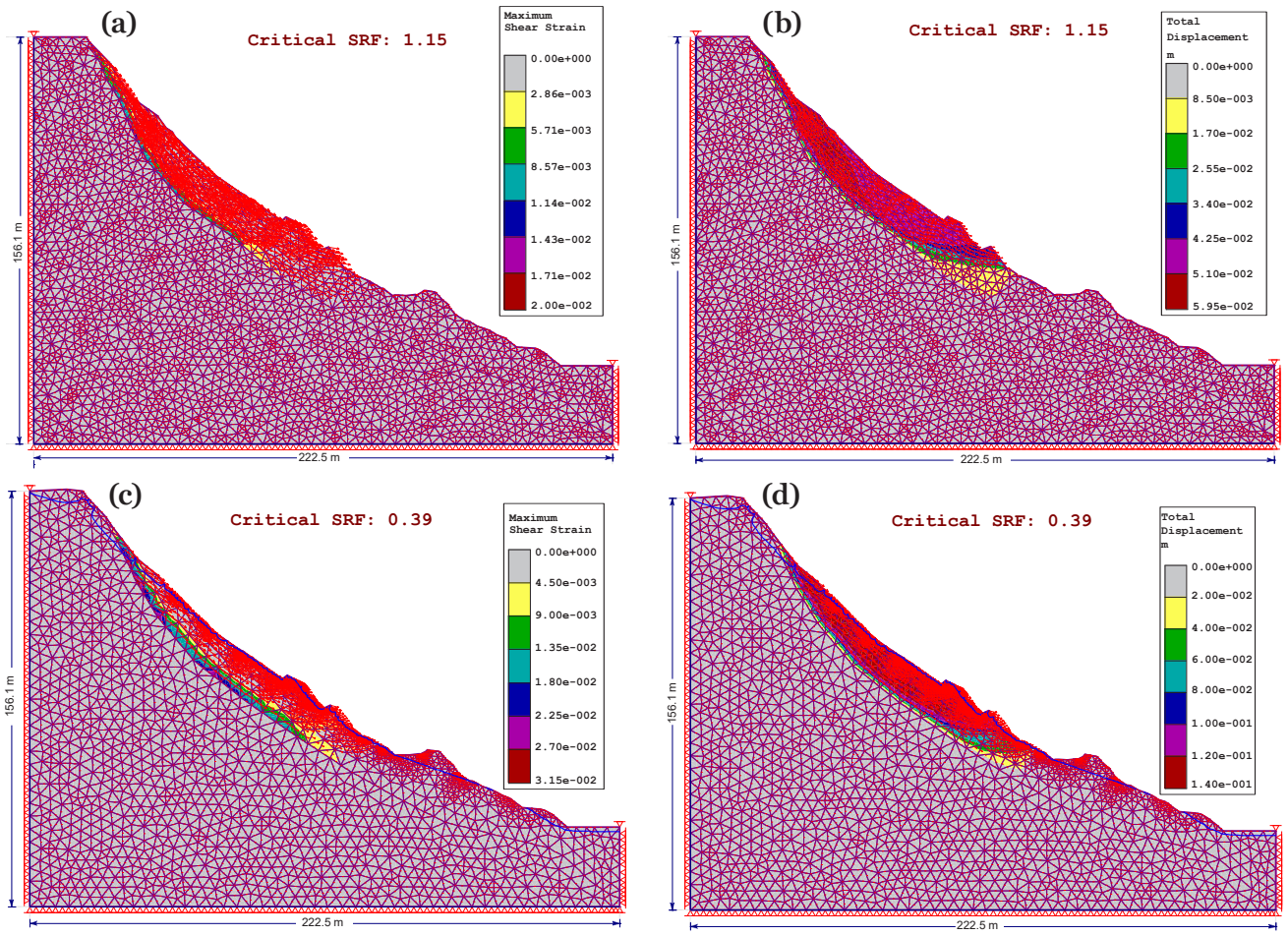

Fig. 10. Maximum deformation vectors at Site-2 under dry conditions: (a) shear strain, (b) total displacement and under saturated conditions: (c) shear strain, (d) total displacement.

saturated conditions (Fig. 10a, c) indicating a 133 % increase in shear strain due to increased pore water pressures within the slope debris mass.

Total displacement contours with deformation vectors from FEM results show the zone of failure, its distribution and intensity, thereby expressing deformation behaviour across the slope. At Site-1, the magnitude of displacement contours illustrates that maximum displacement occurs at the top portion of the free face and gradually diminishes downwards. The maximum displacements for Site-1 and Site-2 under dry conditions are 19.6 mm and 140 mm, respectively (Fig. 9d & Fig. 10d).

Particle Finite Element Method (PFEM)

To ensure the reliability of the numerical results, a series of mesh convergence tests were performed for different mesh sizes of 4.0 m, 3.0 m, 2.0 m, 1.0 m and 0.5 m consecutively to compare the resulting sediment deposition heights (Fig. 11a).

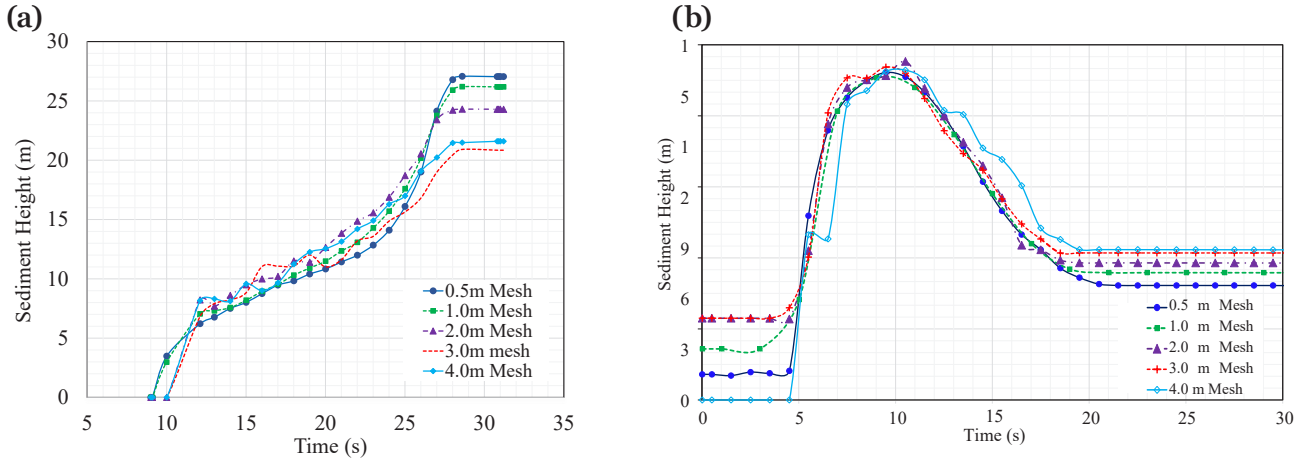

Fig. 11. Temporal variation of sediment deposition height simulated using different mesh sizes in PFEM analysis: (a) at the base of the slope for Site-1 and (b) at the lower road section for Site-2.

The simulation results showed that mesh sizes of 1.0 m and 0.5 m produced nearly identical results, indicating that a 1.0 m mesh provides sufficient resolution for accurately capturing the dynamic debris flow and deposition patterns of the sliding mass, thereby maintaining computational efficiency.

For Site-2, the density, internal friction angle and cohesion of the saturated material were determined to be 2180 kg/m³, 14° and 6 kPa, respectively. A 2D mesh sensitivity analysis was conducted to assess the numerical accuracy of the simulations. By comparing sedimentation height profiles across varying mesh sizes (4.0 m, 2.0 m, 1.0 m and 0.5 m), it was observed that mesh sizes of 0.5 m and 1.0 m yielded nearly identical results (Fig. 11b). The results have confirmed the adequacy of the 1.0 m mesh for optimising the runout dynamics and flow morphology without hindering computational efficiency, which aligns with the recommendations from similar PFEM studies by Cremonesi et al. (2011) and Oñate et al. (2014).

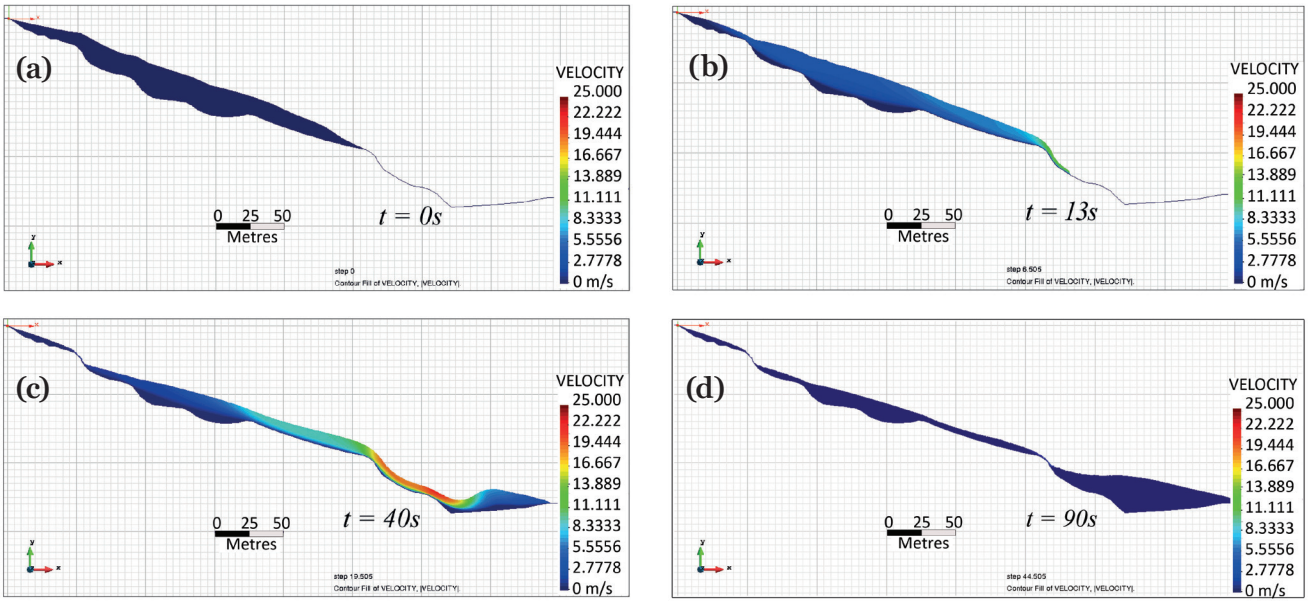

Fig. 12. Progressive post-failure flow stages at Site-1 simulated using 2D-PFEM: (a) t = 0s (b) t = 13s, (c) t = 40s, and (d) t = 90s.

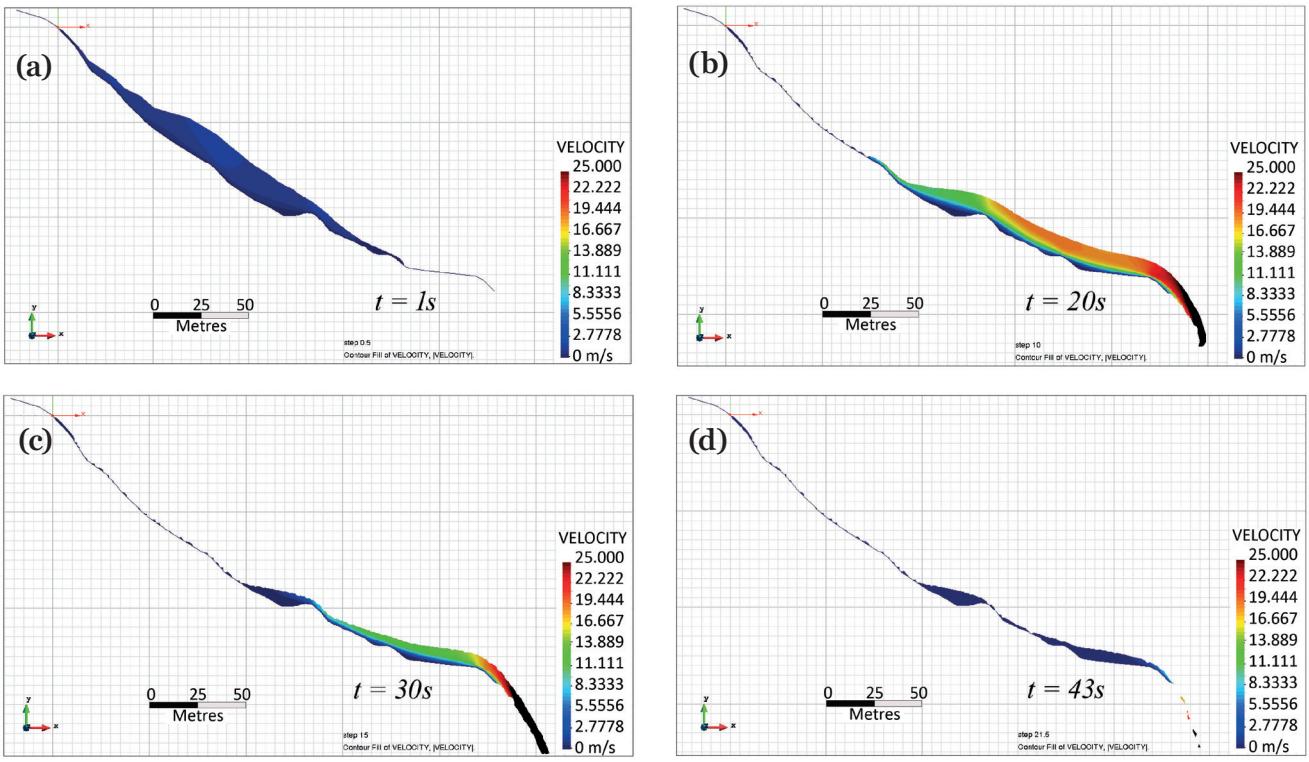

Fig. 13. Progressive post-failure stages at Site-2 simulated using 2D-PFEM: (a) t = 1s, (b) t = 20s, (c) t = 30s, and (d) t = 43s.

The PFEM simulation at Site-1 has assessed both the initiation of failure and the subsequent transport of residual soil with particular emphasis on the Lesser Himalaya of central and western Nepal, where annual rainfall averages approximately 254 mm. The numerical result for this site has provided insights into the landslide dynamics under debris-fluid flow conditions. The debris mass progressively accelerated downslope, reaching a peak velocity of 19.6 m/s before impacting the slope base. The computed runout distance is approximately 425 m from the roadway at the slope crest, which reflects the mobility and energy of the sliding mass. The final deposition profile shows a maximum sediment thickness of 26.1 m at the base of the slope (Fig. 12).

The PFEM analysis for Site-2 was performed in both 2D and 3D configurations, which displayed a realistic simulation of the post-failure conditions. Fig. 13 and Fig. 14 illustrate the time-evolved

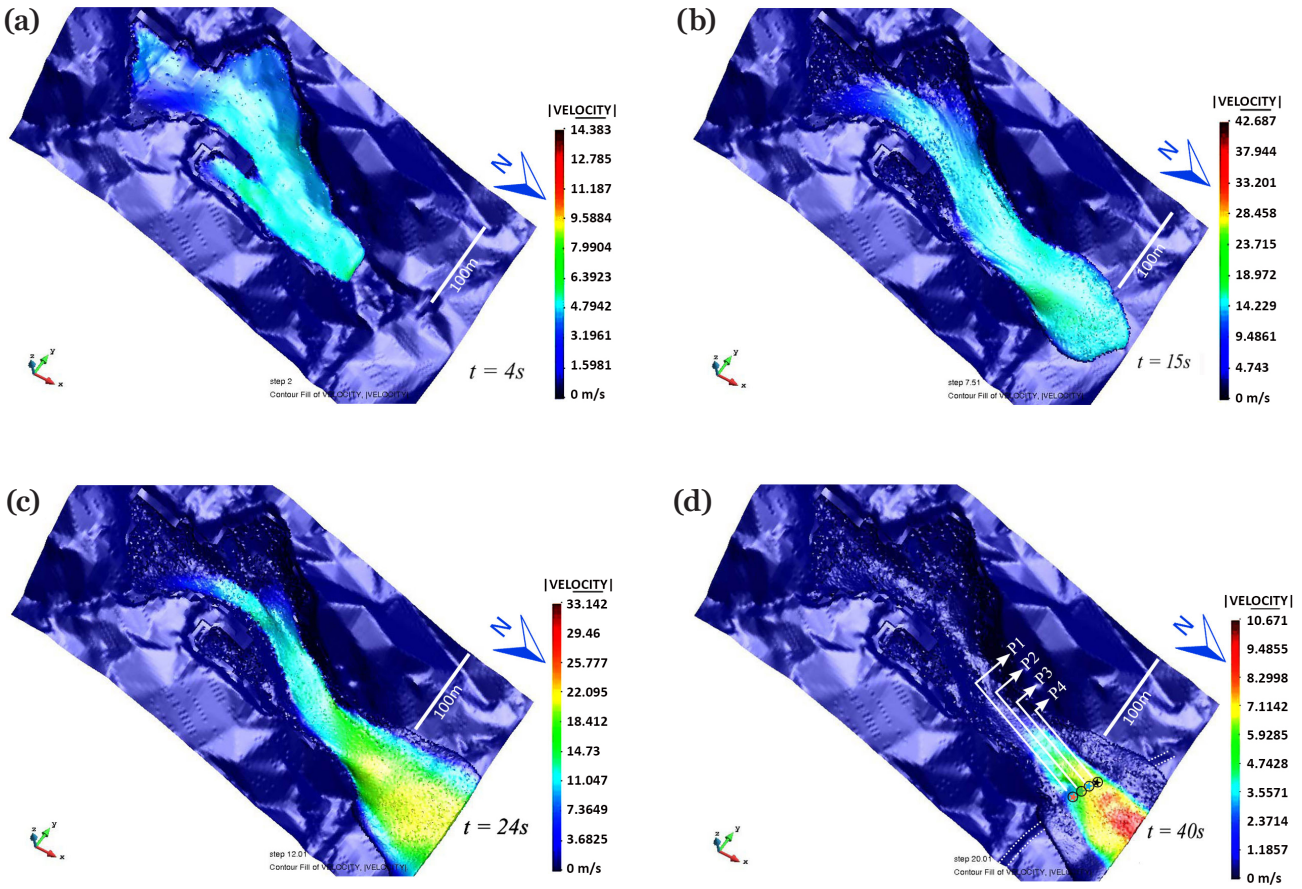

Fig. 14. Progressive post-failure stages at Site-2 simulated using 3D-PFEM: (a) t = 4s, (b) t = 15s, (c) t = 24s and (d) t = 40s.

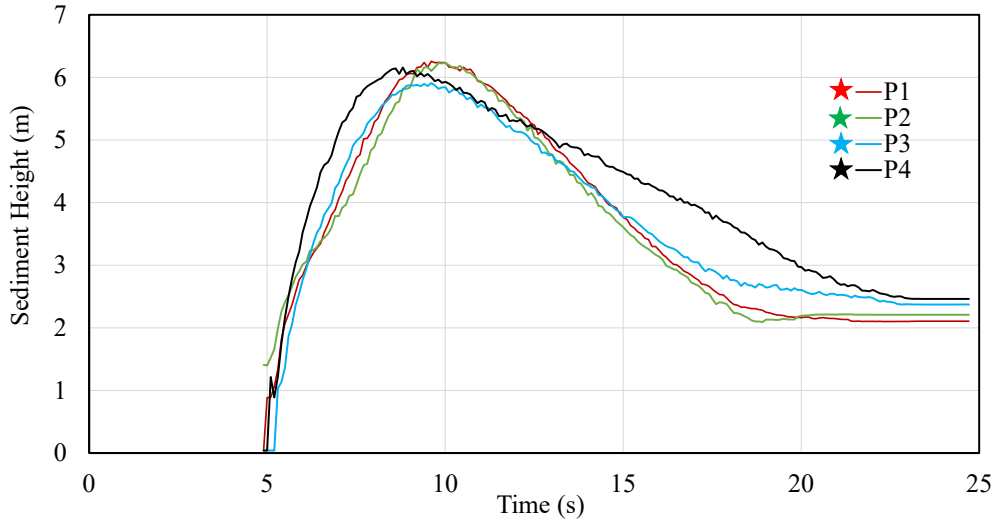

Fig. 15. Temporal evolution of sediment accumulation at four locations along the lower road section of Site-2, based on computed results from the 3D PFEM simulation. (*Notations P1 to P4 correspond to observation points indicated in Fig. 14d*)

progression of the sliding mass, from initial detachment to eventual deposition and spreading at the lower end. A significant accumulation of failed material was observed at the base of the slope where a motorable road was blocked by the debris mass. The simulation results indicated a maximum deposition thickness of approximately 6.2 m at the point of observation along the lower road section (Fig. 15).

Model performance and sensitivity

The cut slope modelling approach effectively predicted FoS and identified potential slip surfaces under varying geological and hydrological conditions using pre-failure analyses via LEM and FEM. The quick estimations from LEM were refined through FEM, which accounted for stress–strain behaviour and complex slope geometries. Post-failure conditions simulated through PFEM successfully reconstructed deformation patterns using site-specific geotechnical inputs. The consistency between pre- and post-failure results aligns well with field observations, validating the reliability and robustness of the adopted modelling techniques.

The results from LEM and FEM analyses demonstrate that changes in GWL have a significant impact on slope stability at both sites. The slopes remained unstable when the GWL was 1.0 m below the surface but became marginally stable between 2.0 and 6.0 m and reached a stability condition when the GWL dropped below 7.0 m with FoS exceeding 1.25. The observed pattern was uniform for both methods at Site-1; however, FEM results at Site-2 remained unstable even when the GWL was below 2.0 m (Fig. 16). The analysis showed that FoS/SRF values increased steadily with groundwater levels lowering down at both locations, which suggests that deeper groundwater levels increase the stability of slopes. Conversely, a rise in GWL due to infiltration during rainfall led to a reduction in FoS. The rise in GWL induces seepage forces which also align in the direction of potential slope movement and augment the contributing factors causing instability (Fredlund et al., 2012). At both sites, increased saturation leads to the loss of matric suction, causing the soil to weaken and become more susceptible to failure (Lu & Godt, 2013). FEM results further indicated that Site-2 is more susceptible to groundwater fluctuations than Site-1.

Site-1 undergoes FoS changes of 40.78 % in LEM and 46.47 % in FEM when transitioning from dry to saturated conditions. Similarly, Site-2 undergoes a change of 61.18 % in LEM and 65.81 % in FEM under the same conditions. The changes in FoS from dry to saturated conditions in both LEM and FEM methods are high and range from 40.78 % to 65.81 % across both sites. Under dry conditions, a change of 3.79 % and 27.32 % occurred in FoS by LEM and FEM at Site-1 and Site-2, respectively, which are dependent on the site-specific geo-material properties (Table 2). Similarly, in saturated conditions, the change in FoS in LEM and FEM for Site-1 and Site-2 are 13.04 % and 36 %, respectively.

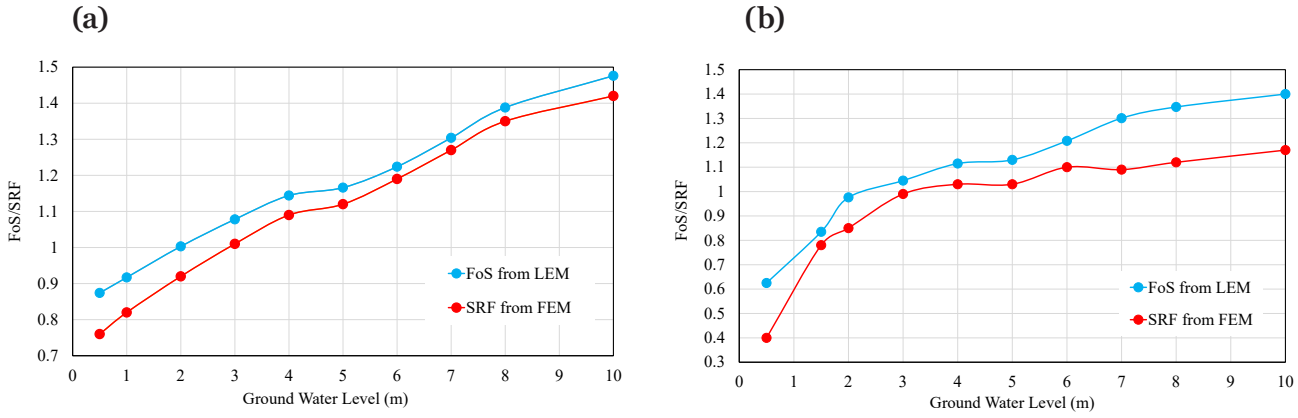

Fig. 16. Comparison of safety factors obtained from LEM and FEM at varying groundwater levels: (a) Site-1 and (b) Site-2.

Table 2. Variation in FoS under dry and saturated conditions for both sites using LEM and FEM methods.

Location	LEM (dry)	LEM (sat.)	% change in LEM (dry & sat.)	FEM (dry)	FEM (sat.)	% change in FEM (dry & sat.)	% change in LEM (dry) & FEM (dry)	% change in LEM (sat.) & FEM (sat.)
Site-1	1.476	0.874	40.78	1.42	0.76	46.47	3.79	13.04
Site-2	1.610	0.625	61.18	1.17	0.40	65.81	27.32	36.00

A comparison of LEM and FEM results under dry conditions revealed a minimal variation of 2.54 % in the safety factor, demonstrating strong agreement between the two methodologies in the absence of groundwater influence. This variation increased slightly to 2.74 % under saturated conditions, indicating that both methods consistently capture the effects of saturation on slope stability. This marginal increase can be attributed to the more complex hydro-mechanical processes accounted for in FEM, including stress redistribution and strain localisation, which are not addressed in LEM (Dawson et al., 1999; Sheng et al., 2003).

Sensitivity analyses of the slopes at both sites were performed to identify the slope parameters that significantly influence the slope stability (Fig. 17). This analysis helps in understanding failure mechanisms, evaluating model robustness, supporting design decisions and optimising the monitoring stages of a slope.

The sensitivity analyses for Site-1 (Fig. 17a) and Site-2 (Fig. 17b) showed that the friction angle (φ) has the most significant influence on slope stability and that an increase in friction angle significantly increases the FoS. Cohesion (c) also has a positive influence on stability, but to a lesser extent. On the other hand, unit weight (γ) has a negative correlation, where an increase in unit weight results in a decrease of FoS. This implies that reducing the soil weight or increasing the frictional resistance can greatly enhance the slope stability at Site-1. From these two analyses, it is observed that the change in FoS is non-linear for friction angle and unit weight but is linear for cohesion. The variation in FoS in both analyses is less than 1 %, indicating a strong agreement.

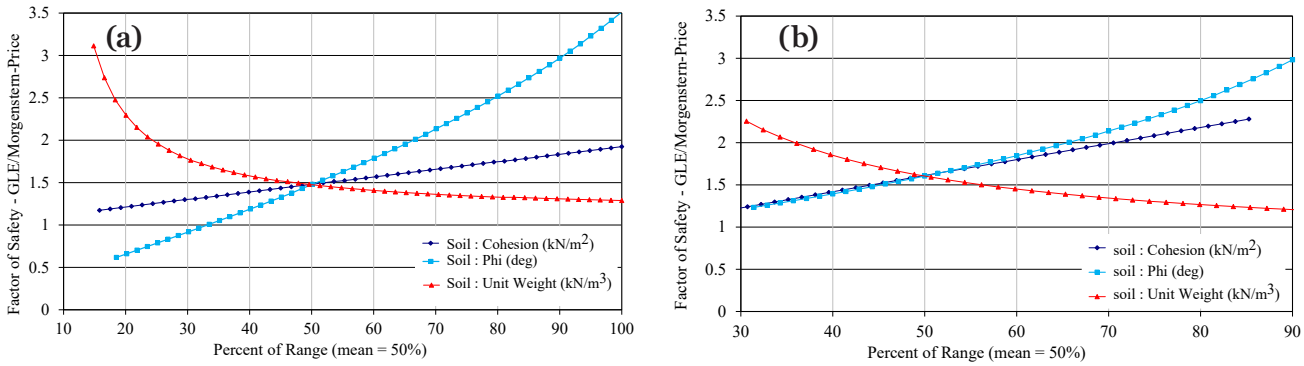

Fig. 17. Sensitivity analysis of slope stability parameters: (a) Site-1 and (b) Site-2.

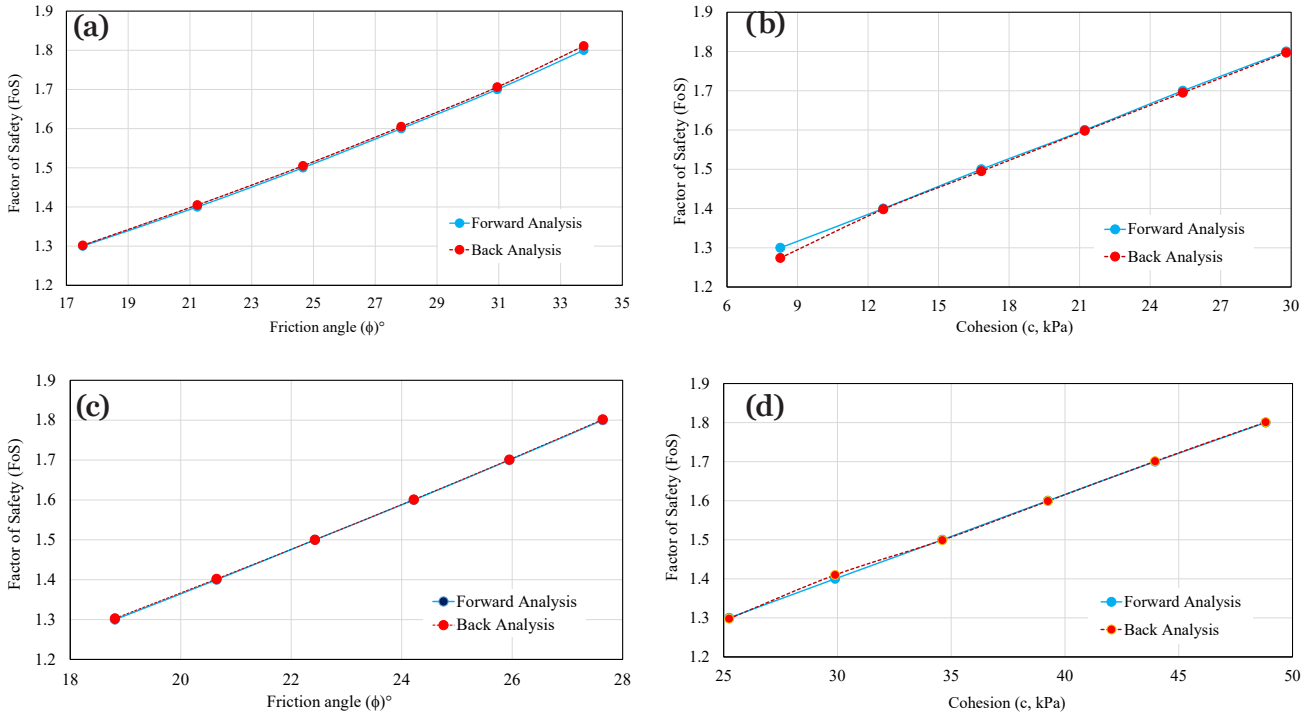

Fig. 18. Evaluation of model consistency through forward and backward analyses under parameter variation: (a) Site-1 with constant cohesion, (b) Site-1 with constant friction angle, (c) Site-2 with constant cohesion and (d) Site-2 with constant friction angle.

The close agreement between forward and back analyses for both modelling sites demonstrated the robustness and reliability of the numerical models (Fig. 18), confirming that the selected geotechnical parameters (c, φ, γ) are well-calibrated and effective in predicting slope stability behaviour under varying conditions.

The maximum shear strain for both slopes was found to be confined at the slip surface, which diminishes gradually towards the ground surface. This shear strain achieved its maximum value under saturated conditions for both slopes and was lower in dry conditions. The increase in shear strain is attributed to elevated pore water pressures that decrease the effective stress within the slope materials. The higher strain values under dry conditions at Site-1 as compared to Site-2 indicated that the soil profile at Site-1 exhibits weaker deformation characteristics, possibly due to lower stiffness and higher water retention or finer soil grains. Site-2 showed lower strain values under dry conditions, which signifies the stable and stiff material behaviour, likely due to its coarse-grained structure and dense packing. Thus, the present study highlights the importance of integrating advanced numerical methods such as FEM for slope stability evaluations, particularly in Lesser Himalayan regions which experience seasonal groundwater fluctuations. The capability of FEM to simulate both stress and deformation makes it well suited for analysing residual soil slopes, which often exhibit progressive failure under saturated conditions.

The pre-failure evaluation of cut slope sites was further simulated using PFEM, with results showing a maximum deposition thickness of 26.1 m at the base of Site-1 and approximately 6.2 m at the lower road section of Site-2. These results are in close agreement with field observations and the damage reports provided by the Department of Roads (DoR), Nepal, thereby validating the model's performance. The consistency between the numerical results and field evidence reinforces the reliability and potential of PFEM for modelling real-world slope failures. Previous researchers have also successfully simulated comparable failure mechanisms in their studies on rapid landslides, debris flows and earth dam failures (Llano-Serna et al., 2016; Zabala & Alonso, 2011).

Validation of model

Validation is essential for establishing the reliability of numerical models in slope stability assessments (e.g., Trucano et al., 2006; Xiong et al., 2009; Fawaz et al., 2014; Kaczmarek & Popielski, 2019). It involves comparing model predictions with field observations or established analytical solutions to ensure the accuracy and reliability of the model outputs (Kaczmarek & Popielski, 2019). This process is crucial for confirming the suitability of models in evaluating slope stability and predicting potential failures. In this study, the validity of the results was enhanced through a comparative analysis of outcomes from LEM, FEM, and PFEM applied to two slides with similar geological settings. The convergence of results among these methods strengthens the overall validity. A similar comparative validation approach was employed by Pradhan & Siddique (2020), using numerical outputs from different methods. The use of slope sections with comparable material properties and boundary conditions across different locations has also been recognised as an effective validation strategy (e.g., Fredlund & Krahn, 1977; Xing, 1988; Griffiths & Marquez, 2007; Mekonnen, 2021). A similar validation approach has been adopted in the present study using a Slide, Phase^2 and PFEM simulations with the same material and boundary conditions.

The safety factors obtained from LEM and FEM for varying groundwater levels at Site-1 and Site-2 were cross-plotted to assess their correlation. The correlation coefficient of the best-fit line quantifies the degree of agreement between the two methods, demonstrating the reliability of the results. A strong correlation reinforces the validity of the derived safety factors (Fig. 19), while discrepancies may indicate methodological limitations or site-specific influences. The findings underscore the importance of implementing complementary analytical approaches in geotechnical solutions.

The computed correlation coefficients of the safety factors derived from the Limit Equilibrium Method (LEM) and the Finite Element Method (FEM) for Site-1 and Site-2 are 0.99 and 0.91, respectively. These values indicate a very strong positive linear relationship between the outputs of the two methodologies. For Site-1, the near-perfect correlation coefficient (R^2=0.99) demonstrates that the safety factors calculated by FEM align closely with those obtained from LEM. This implies that under the given boundary conditions, soil properties, and groundwater regimes, the simplified assumptions in LEM are sufficiently representative of the slope's actual stability conditions captured by FEM, which accounts for more complex stress–strain behaviour and material deformation.

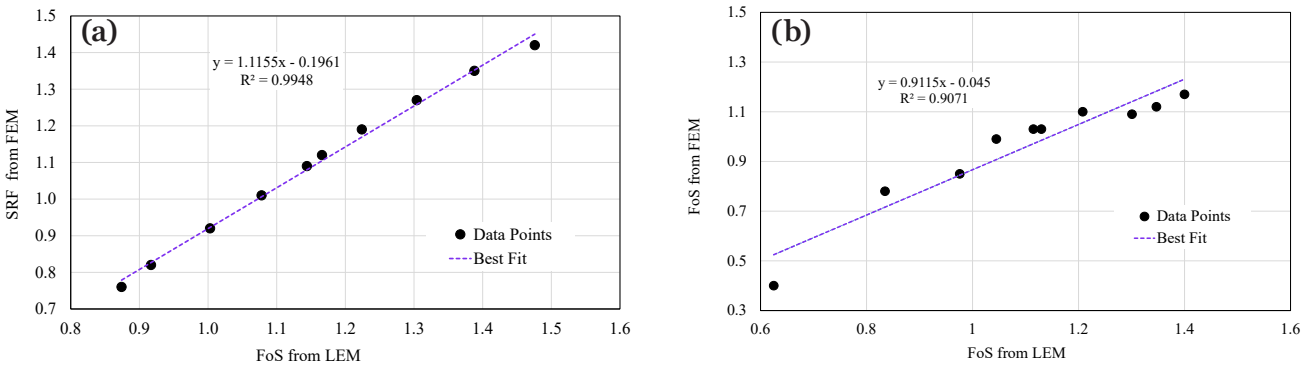

Fig. 19. Correlation between the safety factors derived from the Finite Element Method (FEM; Phase^2) and the Limit Equilibrium Method (LEM; Slide) for (a) Site-1 and (b) Site-2. Linear regression lines and coefficients of determination (R^2) demonstrate the strong consistency between the two modelling approaches.

The correlation coefficient (R^2 = 0.91) at Site-2 is slightly lower than that of Site-1 but still indicates a robust agreement between the two methods. The observed difference could be attributed to site-specific geotechnical complexities such as heterogeneity of material layering, anisotropy, or non-linear deformation behaviour which are better represented in FEM due to its continuum-based formulation. FEM's capability to simulate progressive failure mechanisms, pore pressure redistribution, and localised yielding makes it especially sensitive to such conditions, thereby leading to slight deviations from LEM predictions. Nevertheless, the high correlation coefficients at both sites confirm the mutual consistency and validation of the two modelling approaches in evaluating slope stability. This supports the application of LEM for preliminary assessments or parametric studies while highlighting FEM's strength for more detailed and deformation-based analyses, particularly under complex geological or hydrological conditions.

Conclusions

This study has evaluated the cut slopes in the Lesser Himalaya of Nepal that are often influenced by groundwater saturation together with slope geometry and triggering factors. Pre-failure analyses using the Limit Equilibrium Method (LEM) and Finite Element Method (FEM) revealed that saturation substantially reduces the shear strength of slope material, causing safety factors to attenuate by 40.78–65.81 % when transitioning from dry to saturated conditions. The analysis of the modelling sites showed that slopes remained unstable when groundwater levels were within 1.0 m from the surface, became marginally stable between 2.0 m and 6.0 m, and achieved stable conditions below 7.0 m depths with a factor of safety exceeding 1.3. Closely aligned results from both LEM and FEM results (<10 % variation) and the good agreement between forward and back analyses (<1 % deviation) validate the robustness and reliability of the adopted numerical modelling techniques. The post-failure Particle Finite Element Method (PFEM) simulations quantified the dynamic failure behaviour which computed the debris velocities of 19.6–23 m/s and runout distances of 305–425 m, thereby providing insights into potential impact zones and downstream risks.

An integrated LEM-FEM-PFEM framework has proven to be a suitable approach for analysing slope stability under varying groundwater conditions and identifying critical slope sections. The findings of this research not only decipher failure mechanisms of cut slopes in the Lesser Himalaya but also provide a validated multi-method evaluation in similar geo-environmental settings. The results also deliver valuable scientific and practical insights for designing resilient infrastructure and reducing cut slope failure hazards.

Acknowledgements

We are grateful to the Centre for Numerical Methods in Engineering (CIMNE), Spain for providing an opportunity of a research stay to the first author in acquiring the knowledge of numerical modelling techniques under the Marie Skłodowska-Curie Actions (MSCA) Staff Exchange Project ("LOC3G") funded by the European Commission.

References

Acharya, A. & Dhital, M.R. 2023: Rock mass qualitative stability aspects of cut-slopes in the Lesser Himalaya of central Nepal. Bulletin of Nepal Geological Society, 40: 93–100.

Adhikari, B. R. & Gautam, S. 2022: A review of policies and institutions for landslide risk management in Nepal. Nepal Public Policy Review, 2: 93–112.

Bhattarai, P., Tiwari, B., Marui, H. & Aoyama, K. 2004: Quantitative slope stability mapping with ArcGIS: prioritize highway maintenance. In: Proceedings of ESRI's 24th Annual International User's Conference, San Diego. ESRI.

Bishop, A.W. 1955: The use of the slip circle in the stability analysis of slopes. Géotechnique, 5/1: 7–17. https://doi.org/10.1680/geot.1955.5.1.7

Burman, A., Acharya, S., Sahay, R. & Maity, D. 2015: A comparative study of slope stability analysis using traditional limit equilibrium method and finite element method. Asian Journal of Civil Engineering, 16/4: 467–492.

Cardarelli, E. & Fischanger, F. 2006: 2D data modelling by electrical resistivity tomography for complex subsurface geology. Geophysical Prospecting, 54/2: 121–133.

Cheng, Y.M., Lansivaara, T. & Wei, W.B. 2007: Two-dimensional slope stability analysis by limit equilibrium and strength reduction methods. Computers and geotechnics, 34/3: 137–150.

Chugh, A.K. 2003: On the boundary conditions in slope stability analysis. International journal for numerical and analytical methods in geomechanics, 27/1: 905–926.

Craig, R.F. 2004: Craig's Soil Mechanics (7th ed.). Spon Press, 460 p.

Cremonesi, M., Franci, A. & Perego, U. 2011: A Lagrangian finite element approach for the simulation of the extrusion process in hot metal forming. Computer Methods in Applied Mechanics and Engineering, 200/13-16: 867–882.

Cremonesi, M., Franci, A., Idelsohn, S. & Oñate, E. 2020: A state of the art review of the particle finite element method (PFEM). Archives of Computational Methods in Engineering, 27/5: 1709–1735.

Cruden, D.M. & Varnes, D.J. 1996: Landslide types and processes. In: Turner, A.K. & Schuster, R.L. (eds.): Landslides investigation and mitigation. Transportation research board, US National Research Council. Special Report 247, Washington, DC, Chapter 3: 36–75.

Dahal, R.K. & Hasegawa, S. 2008: Representative rainfall thresholds for landslides in the Nepal Himalaya, Geomorphology, 100/3-4: 429–443. https://doi.org/10.1016/j.geomorph.2008.01.014

Dahal, R.K. 2014: Regional-scale landslide activity and landslide susceptibility zonation in the Nepal Himalaya. Environmental Earth Sciences, 71: 5145–5164. https://doi.org/10.1007/s12665-013-2917-7

Dahal, R.K., Hasegawa, S., Masuda, T. & Yamanaka, M. 2006: Roadside slope failures in Nepal during torrential rainfall and their mitigation. Disaster mitigation of debris flows, slope failures and landslides: 503–514.

Dahal, R.K., Hasegawa, S., Nonomura, A., Yamanaka, M., Dhakal, S. & Paudyal, P. 2008: Predictive modelling of rainfall-induced landslide hazard in the Lesser Himalaya of Nepal based on weights-of-evidence. Geomorphology, 102/3-4: 496–510. https://doi.org/10.1016/j.geomorph.2008.05.041

Dawson, E.M., Roth, W.H. & Drescher, A. 1999: Slope stability analysis by strength reduction. Géotechnique, 49/6: 835–840. https://doi.org/10.1680/geot.1999.49.6.835

Deng, D.P., Li, L. & Zhao, L.H. 2017: Limit equilibrium method (LEM) of slope stability and calculation of comprehensive factor of safety with double strength-reduction technique. Journal of Mountain Science, 14/11: 2311–2324. https://doi.org/10.1007/s11629-017-4537-2

Department of Hydrology & Meteorology (DHM), 2024: Climate Services. Government of Nepal. https://www.dhm.gov.np/climate-services/climate%20reports/monthly-reports

DoR, 2007: Roadside Geotechnical Problems: A Practical Guide to their Solution. Road Maintenance and Development Project, Department of Road (DoR), Government of Nepal: 217 p.

Devkota, K.C., Regmi, A.D., Pourghasemi, H.R., Yoshida, K., Pradhan, B., Ryu, I.C., Dhital, M.R. & Althuwaynee, O.F. 2013: Landslide susceptibility mapping using certainty factor, index of entropy and logistic regression models in GIS and their comparison at Mugling–Narayanghat road section in Nepal Himalaya. Natural hazards, 65: 135–165.

Dhakal, D. & Acharya, I.P. 2019: Slope Stability Analysis of Hill Side Steep Cut Slope and Its Stabilization by the Method Soil Nailing Technique, A Case Study of Narayanghat-Mugling Road Section. In: Proceedings of Institute of Engineering (IOE) Graduate Conference, Nepal.

Dhital, M.R. 2015: Geology of the Nepal Himalaya: regional perspective of the classic collided orogen. Springer: 498 p.

Dikshit, A., Sarkar, R., Pradhan, B., Segoni, S. & Alamri, A.M. 2020: Rainfall induced landslide studies in Indian Himalayan region: a critical review. Applied Sciences, 10/7: 2466. https://doi.org/10.3390/app10072466

Duncan, J.M. & Wright, S.G. 2005: Soil Strength and Slope Stability. John Wiley & Sons Inc., 309 p.

Fan, Q., Lin, J., Sun, W., Lu, J. & Chen, P. 2021: Analysis of Landslide Stability Based on the Morgenstern-Price Method. In E3S Web of Conferences, 299: 02019.

Fawaz, A., Farah, E. & Hagechehade, F. 2014: Slope stability analysis using numerical modelling, American Journal of Civil Engineering, 2/3: 60–67. https://doi.org/10.11648/j.ajce.20140203.11

Fellenius, W. 1936: Calculation of the stability of earth dams. In: Proceedings, 2nd Congress, International Society of Soil Mechanics and Foundation Engineering: 445–462.

Franci, A., Cremonesi, M., Perego, U. & Oñate, E. 2020: A Lagrangian nodal integration method for free-surface fluid flows. Computer Methods in Applied Mechanics and Engineering, 361: 112816.

Fredlund, D.G. & Krahn, J. 1977: Comparison of slope stability methods of analysis. Canadian Geotechnical Journal, 14/3: 429–439. https://doi.org/10.1139/t77-045

Fredlund, D.G., Rahardjo, H. & Fredlund, M.D. 2012: Unsaturated Soil Mechanics in Engineering Practice. John Wiley & Sons: 926 p.

Gansser, A. 1974: Himalaya. Geological Society, London, Special Publications, 4/1: 267–278.

Gerrard, J. 1994: The landslide hazard in the Himalayas: geological control and human action. Geomorphology and Natural Hazards, 10: 221–230. https://doi.org/10.1016/B978-0-444-82012-9.50019-0

Griffiths, D. V. & Marquez, R. 2007: Three-dimensional slope stability analysis by elasto-plastic finite elements. Geotechnique, 57/6: 537–546.

Griffiths, D.V. & Lane, P.A. 1999: Slope stability analysis by finite elements. Géotechnique, 49/3: 387–403. https://doi.org/10.1680/geot.1999.49.3.387

Groppo, C., Rolfo, F., Tamang, S. & Mosca, P. 2023: Lithostratigraphy, Petrography Lesser and Metamorphism Himalayan Sequence. Himalaya, Dynamics of a Giant 2: Tectonic Units and Structure of the Himalaya: 157–188.

Haigh, M. & Rawat, J.S. 2011: Landslide causes: Human impacts on a Himalayan landslide swarm. Belgeo, Revue belge de géographie, 3–4: 201–220.

Hasegawa, S., Dahal, R.K., Yamanaka, M., Bhandary, N.P., Yatabe, R. & Inagaki, H. 2009: Causes of large-scale landslides in the Lesser Himalaya of central Nepal. Environmental Geology, 57: 1423–1434. https://doi.org/10.1007/s00254-008-1420-z

Hearn, G.J. 2011: Slope engineering for mountain roads. Geological Society of London: 223 https://doi.org/10.1144/EGSP24

Hearn, G.J. & Shakya, N.M. 2017: Engineering challenges for sustainable road access in the Himalayas. Quarterly Journal of Engineering Geology and Hydrogeology, 50/1: 69–80.

Hungr, O., Leroueil, S. & Picarelli, L. 2014: The Varnes Classification of Landslide Types, an Update. Landslides, 11: 167–194. https://doi.org/10.1007/s10346-013-0436-y

Idelsohn, S.R., Marti, J., Limache, A. & Oñate, E. 2008: Unified Lagrangian formulation for elastic solids and incompressible fluids: application to fluid–structure interaction problems via the PFEM. Computer Methods in Applied Mechanics and Engineering, 197/19–20: 1762–1776.

Idelsohn, S.R. & Onate, E. 2010: The challenge of mass conservation in the solution of free-surface flows with the fractional-step method: Problems and solutions. International Journal for Numerical Methods in Biomedical Engineering, 26/10: 1313–1330.

Janbu, N. 1954: Application of composite slip surfaces for stability analysis. European Conference on Stability of Earth Slopes, 3: 43–49.

Kaczmarek, L.D. & Popielski, P. 2019: Selected components of geological structures and numerical modelling of slope stability. Open Geosciences, 11/1: 208–218.

Kharel, G. & Acharya, I.P. 2017: Stability Analysis of Cut-slope: A case study of Kathmandu-Nijgadh Fast track. In: Proceedings of Institute of Engineering (IOE) Graduate Conference, 5: 171–174.

Khatri, S. & Acharya, I. P. 2019: Stability Analysis of Road-Cut slope: A Case Study of Kanti Lokpath. In: KEC Conference: 205–208.

Komadja, G.C., Pradhan, S.P., Roul, A.R., Adebayo, B., Habinshuti, J.B., Glodji, L.A. & Onwualu, A.P. 2020: Assessment of stability of a Himalayan road cut slope with varying degrees of weathering: A finite-element-model-based approach. Heliyon, 6/11. https://doi.org/10.1016/j.heliyon.2020.e05297

Llano-Serna, M.A., Oñate, E. & Idelsohn, S. 2016: Particle finite element method for the simulation of large deformation landslides. Computers and Geotechnics, 74: 118–126.

Loke, M.H. 2004: Tutorial: 2-D and 3-D electrical imaging surveys. Geotomo Software, Res2dinv 3.5 Software. 136 p.

Loke, M.H., Chambers, J.E., Rucker, D.F., Kuras, O. & Wilkinson, P.B. 2013: Recent developments in the direct-current geoelectrical imaging method. Journal of Applied Geophysics, 95: 135–156.

Lowe, J. & Karafiath, L. 1965: Slope stability analysis by the moment method. Proceedings of the American Society of Civil Engineers, 91: 1–27.

Lu, N. & Godt, J.W. 2013: Hillslope hydrology and stability. Cambridge University Press: 458 p.

Marc, O., Behling, R., Andermann, C., Turowski, J.M., Illien, L., Roessner, S. & Hovius, N. 2019: Long-term erosion of the Nepal Himalayas by bedrock landsliding: The role of monsoons, earthquakes and giant landslides. Earth Surface Dynamics, 7/1: 107–128. https://doi.org/10.5194/esurf-7-107-2019

Martin, R.P. 2001: The design of remedial works to the Dharan–Dhankuta road, East Nepal. Geological Society, London, Engineering Geology Special Publications, 18/1: 197–204 https://doi.org/10.1144/GSL.ENG.2001.018.01.28

Maskey, S. 2016: A Case Study of the Krishna Bhir slope failure disaster: past and present scenario at a glance. International journal of Rock engineering and Mechanics, 2: 1–11.

Matthews, C., Farook, Z. & Helm, P. 2014: Slope stability analysis–limit equilibrium or the finite element method. Ground Engineering, 48/5: 22–28.

Mekonnen, F.A. 2021: Performance evaluation of geometric modification on the stability of road cut slope using FE Based plaxis software. In Landslides. IntechOpen. https://doi.org/10.5772/intechopen.99633

Morgenstern, N.R. & Price, V.E. 1965: The analysis of the stability of general slip surfaces. Geotechnique, 15/1: 79–93.

Morgenstern, N.R. & Sangrey, D.A. 1978: Methods of stability analysis. Landslides: analysis and control, Transportation Research Board Special Report, 176, Washington, D.C.: 155–171.

Nian, T.K., Huang R.Q., Wan, S.S. & Chen, G.Q. 2012: Three-dimensional strength-reduction finite element analysis of slopes: geometric effects. Canadian Geotechnical Journal, 49/5: 574–588. https://doi.org/10.1139/t2012-014

Oñate, E., Celigueta, M.A., Idelsohn, S.R., Rossi, R. & Suárez, B. 2011: Advances in the particle finite element ethod (PFEM) for solving fluid–soil–structure interaction problems in engineering. Advances in Computational Mechanics: 1–30.

Oñate, E., Franci, A. & Carbonell, J.M. 2014: A particle finite element method (PFEM) for coupled thermal analysis of quasi and fully incompressible flows and fluid-structure interaction problems. In Numerical Simulations of Coupled Problems in Engineering, Springer International Publishing: 129–156.

Oñate, E., Idelsohn, S.R., Del Pin, F. & Aubry, R. 2004: The particle finite element method–an overview. International Journal of Computational Methods, 1/2: 267–307.

Panda, S.D., Kumar, S., Pradhan, S.P., Singh, J., Kralia, A. & Thakur, M. 2023: Effect of groundwater table fluctuation on slope instability: a comprehensive 3D simulation approach for Kotropi landslide, India. Landslides, 20/3: 663–682.

Pant, J.R. & Acharya, I.P. 2021: Stability Analysis of Road-cut Slope: A Case Study of Jiling Landslide along the Galchi-Trishuli-Mailung-Syaprubeshi Rasuwagadi Road. In: Proceedings of 9th Institute of Engineering (IOE) Graduate Conference, Institute of Engineering, Tribhuvan University, Nepal, 9: 9–15.

Panthi, K.K. 2006: Analysis of engineering geological uncertainties related to tunnelling in Himalayan rock mass conditions (PhD dissertation), Trondheim, Norway: Department of Geology and Mineral Resources Engineering, Norwegian University of Science and Technology.

Panthi, K.K. 2021: Assessment on the 2014 Jure Landslide in Nepal – a disaster of extreme tragedy. IOP Conference Series: Earth and Environmental Science. 833. 012179. https://doi.org/10.1088/1755-1315/833/1/012179

Pathak, D. 2014: Geohazard assessment along the road alignment using remote sensing and GIS: Case study of Taplejung-Olangchunggola-Nangma road section, Taplejung district, east Nepal. Journal of Nepal Geological Society, 47/1: 47–56.

Pathak, D. 2016: Knowledge based landslide susceptibility mapping in the Himalayas. Geoenvironmental Disasters, 3: 1–11. https://doi.org/10.1186/s40677-016-0042-0

Phuyal, B. & Thapa, P.B. 2023: Failure mechanism of large-scale landslide in the central Nepal Himalaya. Journal of Nepal Geological Society,

66: 37–52. https://doi.org/10.3126/jngs.v66i01.57921

Phuyal, B., Acharya, M.S. & Thapa, P.B. 2025; Landslide Size-Frequency Distribution and Factor Effects on Susceptibility Modelling in the Himalayan Region, Central Nepal. Geotechnical and Geological Engineering, 43/1: 55. https://doi.org/10.1007/s10706-024-03014-w

Phuyal, B., Thapa, P.B. & Devkota, K.C. 2022: Characterization of large-scale landslides and their susceptibility evaluation in central Nepal Himalaya. Journal of Nepal Geological Society, 63/01: 109–122. https://doi.org/10.3126/jngs.v63i01.50846

Pokharel, R.P., Khanal, N.R. & Paudel, B. 2024: Landslide Susceptibility Analysis in Kaski District, Nepal: Using Remote Sensing Technique with Intensive Field Verification. https://doi.org/10.21203/rs.3.rs-4687294/v1

Poudyal, A., Dahal, A., Shrestha, J. & Timilsina, M. 2024: Cut Slope Stability Analysis on Terrain with Slope at Besishahar, Lamjung. International Journal on Engineering Technology, 1/2: 230–249.

Pradhan, S., Toll, D.G., Rosser, N.J. & Brain, M.J. 2022: An investigation of the combined effect of rainfall and road cut on landsliding. Engineering Geology, 307, 106787. https://doi.org/10.1016/j.enggeo.2022.106787

Pradhan, S.P. & Siddique, T. 2020: Stability assessment of landslide-prone road cut rock slopes in Himalayan terrain: a finite element method based approach. Journal of Rock Mechanics and Geotechnical Engineering, 12/1: 59–73.

Pudasaini, S.P., Mergili, M., Lin, Q. & Wang, Y. 2024: Dynamic simulation of rock-avalanche fragmentation. Journal of Geophysical Research: Earth Surface, 129(9), e2024JF007689.

Rahman, A.U., Khan, A.N. & Collins, A.E. 2014: Analysis of landslide causes and associated damages in the Kashmir Himalayas of Pakistan. Natural Hazards, 71: 803–821. https://doi.org/10.1007/s11069-013-0918-1

Rawat, D.S. & Sharma, S. 1997: The development of a road network and its impact on the growth of infrastructure: a study of Almora District in the Central Himalaya. Mountain Research and Development: 117–126.

Ray, R.L. & De Smedt, F. 2009: Slope stability analysis on a regional scale using GIS: a case study from Dhading, Nepal. Environmental Geology, 57, 1603–1611.

Regmi, A.D., Dhital, M.R., Zhang, J.Q., Su, L.J. & Chen, X.Q. 2016: Landslide susceptibility assessment of the region affected by the 25 April 2015 Gorkha earthquake of Nepal. Journal of Mountain Science, 13: 1941–1957.

Regmi, A.D., Yoshida, K., Dhital, M.R. & Devkota, K. 2013: Effect of rock weathering, clay mineralogy, and geological structures in the formation of large landslide, a case study from Dumre Besei landslide, Lesser Himalaya Nepal. Landslides, 10: 1–13. https://doi.org/10.1007/s10346-011-0311-7

Robson, E., Agosti, A., Utili, S. & Milledge, D. 2022: A methodology for road cutting design guidelines based on field observations. Engineering Geology, 307, 106771. https://doi.org/10.1016/j.enggeo.2022.106771

Robson, E., Pradhan, S. & Toll, D. 2024: A field study on the stability of road cut slopes in Nepal. In: Geo-Resilience 2023 Conference, Cardiff, Wales, ISSMGE Online Library. https://doi.org/10.53243/Geo-Resilience-2023-1-8

Sapkota, B. & Timilsina, M. 2024: Road Side Slope Stabilization Using Ground Water Management at Far-Western Nepal. Asian Journal of Engineering Geology, 1 (Special Issue):17–18.

Sarma, S.K. 1973: Stability analysis of embankments and slopes. Geotechnique, 23/3: 423–433.

Schuster, M. & Hübl, J. 1995: Impact of road construction on the Pokhara-Baglung highway, Kaski district, Nepal. Sustainable reconstruction of highland and headwater regions: 175–182.

Sharma, L.K., Umrao, R.K., Singh, R., Ahmad, M. & Singh, T.N. 2017: Geotechnical characterization of road cut hill slope forming unconsolidated geo-materials: a case study. Geotechnical and Geological Engineering, 35: 503–515.

Sheng, D., Smith, D.W., W. Sloan, S. & Gens, A. 2003: Finite element formulation and algorithms for unsaturated soils. Part II: Verification and application. International Journal for Numerical and Analytical Methods in Geomechanics, 27/9: 767–790.

Shrestha, D.P., Zinck J.A. & Van, R.E. 2004: Modelling land degradation in the Nepalese Himalaya. Catena, 57/2: 135–156. https://doi.org/10.1016/j.catena.2003.11.003

Shrestha, K.K., Paudyal, K.R. & Thapa, P.B. 2023: Numerical modelling of cut-slope stability in the Lesser Himalayan terrain of west-central Nepal. Journal of Nepal Geological Society, 66: 75–90. https://doi.org/10.3126/jngs.v66i01.57933

Silwal, B.R., Gyawali, B.R. & Yoshida, K. 2024: Geochemical and mineralogical analysis of low-

grade metamorphic rocks and their response to shallow landslide occurrence in Central Nepal. Geoenvironmental Disasters, 11/1: 37.

Singh, A.K. 2009: Causes of slope instability in the Himalayas. Disaster Prevention and Management: An International Journal, 18/3: 283–298. https://doi.org/10.1108/09653560910965646

Singh, H.O., Ansari, T.A., Singh, T.N. & Singh, K.H. 2020: Analytical and numerical stability analysis of road cut slopes in Garhwal Himalaya, India. Geotechnical and Geological Engineering, 38: 4811–4829. https://doi.org/10.1007/s10706-020-01329-y

Singh, R., Umrao, R.K. & Singh, T.N. 2014: Stability evaluation of road-cut slopes in the Lesser Himalaya of Uttarakhand, India: conventional and numerical approaches. Bulletin of Engineering Geology and the Environment, 73: 845–857.

Singh, T.N., Gulati, A., Dontha, L. & Bhardwaj, V. 2008: Evaluating cut slope failure by numerical analysis–a case study. Natural Hazards, 47: 263–279. https://doi.org/10.1007/s11069-008-9219-5

Spencer, E. 1967: A method of analysis of the stability of embankments assuming parallel interslice forces. Géotechnique, 17: 11–26. https://doi.org/10.1680/geot.1967.17.1.11

Sutejo, Y. & Gofar, N. 2015: Effect of area development on the stability of cut slopes. Procedia Engineering, 125: 331–337.

Terzaghi, K. 1943: Theoretical Soil Mechanics. John Wiley & Sons: 526 p.

Thapa, P.B. 2015: Occurrence of landslides in Nepal and their mitigation options. Journal of Nepal Geological Society, 49: 17–28. https://doi.org/10.3126/jngs.v49i1.23138

Thapa, P.B., Phuyal, B. & Shrestha, K.K. 2023: Spatial variability of slope movements in central and western Nepal Himalaya: Evaluating large-scale landslides to cut-slopes. Journal of Nepal Geological Society, 65: 183–194. https://doi.org/10.3126/jngs.v65i01.57777

Trucano, T.G., Swiler, L.P., Igusa, T., Oberkampf, W.L. & Pilch, M. 2006: Calibration, validation, and sensitivity analysis: What's what. Reliability Engineering & System Safety., 91/10-11: 1331–1357. https://doi.org/10.1016/j.ress.2005.11.031

Upreti, B.N. & Dhital, M. 1996: Landslide studies and management in Nepal. ICIMOD, Nepal: 87 p.

Upreti, B.N. 1999: An overview of the stratigraphy and tectonics of the Nepal Himalaya. Journal of Asian Earth Sciences, 17/5–6: 577–606. https://doi.org/10.1016/S1367-9120(99)00047-4

USACE, 2003: Engineering and Design: Slope stability, Engineer Manual 11102-2-1902.

Varnes, D.J. 1958: Landslide types and processes. Landslides and engineering practice, 24: 20–47.

Varnes, D.J. 1978: Slope movement types and processes. Special report, 176: 11–33.

Vuillez, C., Tonini, M., Sudmeier-Rieux, K., Devkota, S., Derron, M.H. & Jaboyedoff, M. 2018: Land use changes, landslides and roads in the Phewa Watershed, Western Nepal from 1979 to 2016. Applied Geography, 94: 30–40.

Wyllie, D.C. & Mah, C. 2004: Rock Slope Engineering. 4th Ed. The Institution of Mining and Metallurgi London, 456 p.

Xing, Z. 1988: Three dimensional stability analysis of concave slopes in plan view. Journal of Geotechnical Engineering, 114/6: 658–671.

Xiong, Y., Chen, W., Tsui, K-L. & Apley, D.W. 2009: A better understanding of model updating strategies in validating engineering models. Computer methods in applied mechanics and engineering, 198/15–16: 1327–1337. https://doi.org/10.1016/j.cma.2008.11.023

Zabala, F. & Alonso, E.E. 2011: Progressive failure of Aznalcóllar dam using the finite element method. Géotechnique, 61/9: 795–808.

Zheng, H. 2012: A three-dimensional rigorous method for stability analysis of landslides. Engineering Geology, 145: 30–40.

Zheng, W., Zhuang, X., Tannant, D.D., Cai, Y. & Nunoo, S. 2014: Unified continuum/discontinuum modeling framework for slope stability assessment. Engineering Geology, 179: 90–101.